Trace element geochemistry of K-rich impact spherules from howardites

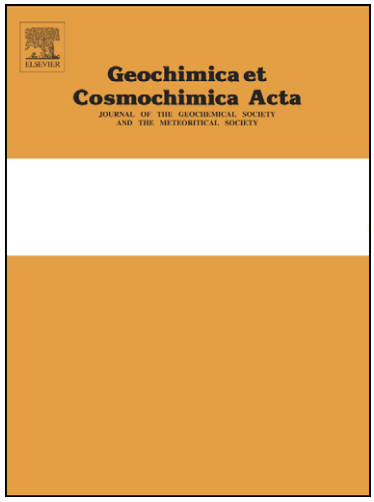

Trace element geochemistry of K-rich impact spherules from howardites

Jean-Alix Barrat, Akira Yamaguchi, Richard C. Greenwood, Claire Bollinger, Marcel Bohn, Ian A. Franchi

PII: S0016-7037(09)00450-5
DOI: 10.1016/j.gca.2009.06.033
Reference: GCA 6368

To appear in: *Geochimica et Cosmochimica Acta*

Received Date: 2 February 2009
Accepted Date: 26 June 2009

Please cite this article as: Barrat, J-A., Yamaguchi, A., Greenwood, R.C., Bollinger, C., Bohn, M., Franchi, I.A., Trace element geochemistry of K-rich impact spherules from howardites, *Geochimica et Cosmochimica Acta* (2009), doi: 10.1016/j.gca.2009.06.033

Trace element geochemistry of K-rich impact spherules from howardites

By

Jean-Alix Barrat[1,2], Akira Yamaguchi[3], Richard C. Greenwood[4], Claire Bollinger[1,2], Marcel Bohn[1,2] and Ian A. Franchi[4].

1: Université Européenne de Bretagne.

2: Université de Brest, CNRS UMR 6538 (Domaines Océaniques), I.U.E.M., Place Nicolas Copernic, 29280 Plouzané Cedex, France. E-Mail: barrat@univ-brest.fr.

3: Antarctic Meteorite Research Center, National Institute of Polar Research, 10-3 Midoricho, Tachikawa, Tokyo 190-8518, Japan.

4: PSSRI, The Open University, Walton Hall, Milton Keynes MK7 6AA, United Kingdom.

Submitted to *Geochim. Cosmochim. Acta*, 2/2/09
Revised version

Abstract

The howardite-eucrite-diogenite (HED) achondrites are a group of meteorites that probably originate from the asteroid Vesta. Howardites are complex polymict breccias that sometimes contain, in addition to various rock debris, impact melt glasses which show an impressive range of compositions. In this paper we report on the geochemistry and O isotopes of a series of 6 Saharan polymict breccias (4 howardites and 2 polymict eucrites), and on the trace element abundances of high-K impact spherules found in two of them, Northwest Africa (NWA) 1664 and 1769, which are likely paired.

The high-K impact spherules found in the howardites NWA 1664 and NWA 1769 display remarkable trace element patterns. Compared to eucrites or howardites, they all show prominent enrichments in Cs, Rb, K, Li and Ba, strong depletion in Na, while the REE and other refractory elements are unfractionated. These features could not have been generated during impact melting of their host howardites, nor other normal HED target materials. The involvement of Na-poor rocks, and possibly rocks of granitic composition, appears likely. Although these lithologies cannot be well constrained at present, our results demonstrate that the surface of Vesta is certainly more diverse than previously thought. Indeed, despite the large number of available HED meteorites (about 1000 different meteorites), the latter are probably not sufficient to describe the whole surface of their parent body.

1. Introduction

4-Vesta, the second largest object by mass in the asteroid belt, is probably the parent body of the most abundant group of achondrites, namely the howardite, eucrite, and diogenite (HED) suite (e.g., McCord et al., 1970; Drake, 2001). Eucrites are basaltic or gabbroic rocks that formed as lava flows or intrusions. They are generally regarded as being samples of the upper crustal lithologies of their parent body. Diogenites are orthopyroxene-rich cumulates, and are generally believed to sample deeper structural levels, but this is presently a matter of discussion (Barrat et al., 2006, 2008). Most eucrites and diogenites record a complex post crystallization history. These rocks were extensively brecciated and locally melted by meteorite impacts. Therefore, eucrites and diogenites are generally breccias consisting of a mixture of crystal debris and rock fragments. Howardites are more complex breccias, composed predominantly of both eucritic and diogenitic clasts (Mittlefehldt et al., 1998).

Howardites and polymict eucrites commonly contain impact melt clasts (e.g., Noonan, 1974; Labotka and Papike, 1980; Fuhrman and Papike, 1981; Mittlefehldt and Lindstrom, 1997), and less frequently impact glass beads (fig. 1). The petrography and the geochemistry of these glasses have recently been reinvestigated, with at least two types of mafic spherules identified in howardite breccias (Barrat et al., 2009a). Firstly, low-K impact glasses (Mg# (=100 x Mg/(Mg+Fe), atomic) from 41 to 72, with K_2O generally less than 0.1 wt%) have been analyzed in Bununu, Kapoeta, Yamato (Y-) 7308 and Y-791208. They are chemically similar to howardites or eucrites, and are formed by melting of an ordinary HED target with negligible effects of impact induced vapor fractionation (e.g., Noonan, 1974; Yagi et al., 1978; Klein and Hewins, 1979: Noonan et al., 1980; Delaney et al., 1982; Ikeda and Takeda, 1984). Secondly, mafic glasses found in Malvern (Noonan, 1974; Desnoyers and Jérome, 1977), Macibini (Buchanan et al., 2000), Northwest Africa (NWA) 1664 (e.g., Kurat et al.,

2003), NWA 1769 and LAP 04838 (Barrat et al., 2009a) display a range of Mg#-values similar to the previous K-poor glasses (Mg# from 32 to 73), but are unusually K-rich, with K_2O concentrations ranging from 0.15 to 2.33 wt%. These K-abundances are much higher than the values generally found in HED meteorites, which in most cases contain significantly less than 0.1 wt% K_2O. Such high K abundances indicate that these impact spherules could not have formed from any known HED lithology. Barrat et al. (2009a) have shown that the behavior of K in these glasses cannot be explained by a projectile contribution, selective alkali vaporization/condensation processes, or by terrestrial contamination. More likely, the high K abundances measured in some impact spherules indicate that some K-rich lithologies were present in the fused target materials. The occurrence of granitic (or felsic) glasses in the Yamato 791073 breccia (Takeda, 1986) and in a NWA 1664 spherule (Barrat et al., 2009a) strongly strengthens this interpretation.

The high-K glasses found in howardites are particularly attractive from a geochemical point of view. Since impact glasses record some of the geochemical features of their source materials and in some instances could have been ballistically transported over large distances, they can potentially provide a complementary view of the chemical composition of the rocks exposed on Vesta. In this paper, we report on the trace element abundances of the unusual high-K glasses found in NWA 1664 and NWA 1769. In addition to NWA 1664 and NWA 1769, we have studied a further two howardites and two polymict eucrites in order to assess whether there are any geochemical features unique to the two spherule-bearing samples.

2. Analytical procedures

2.1 Bulk rock compositions

Meteorite fragments were powdered using a boron carbide mortar and pestle. Minor and trace element concentrations were measured at the Institut Universitaire Europeen de la Mer (IUEM), Plouzané, by ICP-MS (inductively coupled plasma-mass spectrometry) using a Thermo Element 2 spectrometer following the procedures described by Barrat et al. (2007). Based on standard measurements and sample duplicates, concentration reproducibility is generally much better than 5 %.

2.2 Oxygen isotopes

Oxygen isotope analyses were carried out using an infrared laser fluorination system at The Open University (Miller et al., 1999). Aliquots (~2 mg), taken from larger batches of homogenized powdered samples (section 3.1), were analyzed both untreated and after leaching in 6M HCl for 30 minutes. To maximize yields and decrease the risk of cross-contamination the powdered samples were fused in vacuum to form a glass bead prior to fluorination. O_2 was liberated by heating the glass beads using an infrared CO_2 laser (10.6 μm) in the presence of 210 torr of BrF_5. After fluorination, the O_2 released was purified by passing it through two cryogenic nitrogen traps and over a bed of heated KBr. O_2 was analyzed using a Micromass Prism III dual inlet mass spectrometer. Published system precision (1σ) (Miller et al., 1999), based on replicate analyses of international (NBS-28 quartz, UWG-2 garnet) and internal standards, is approximately ±0.04‰ for $\delta^{17}O$; ±0.08‰ for $\delta^{18}O$; ±0.02‰ for $\Delta^{17}O$. More recent replicate analyses of the UWG-2 garnet standard gave the following values for system precision (1σ): ±0.03‰ for $\delta^{17}O$; ±0.07‰ for $\delta^{18}O$; ±0.01‰ for $\Delta^{17}O$. The quoted precision (1σ) for the howardite samples is based on replicate

analyses. Oxygen isotope analyses are reported in standard δ-notation where $\delta^{18}O$ has been calculated as: $\delta^{18}O = ((^{18}O/^{16}O_{sample} / {}^{18}O/^{16}O_{ref})-1) \times 1000$ and similarly for $\delta^{17}O$ using $^{17}O/^{16}O$ ratio. $\Delta^{17}O$ has been calculated using the linearized format of Miller (2002): $\Delta^{17}O = 1000 \ln (1+ (\delta^{17}O /1000)) – \lambda 1000 \ln(1+ (\delta^{18}O /1000))$ where $\lambda = 0.5247$.

2.3 *In-situ* trace element abundances

Glass spherules located within polished thick-sections were first analyzed for major and minor elements by electron microprobe at Ifremer, Plouzané, using a Cameca SX100 instrument. The results of this work were previously reported by Barrat et al. (2009a). Trace elements were subsequently determined by laser ablation inductively coupled plasma mass spectrometry (LA-ICPMS) at Institut Universitaire Européen de la Mer, Plouzané. The analyses were performed under a He atmosphere using an Excimer (193 nm wavelength) laser ablation system (Geolas Pro102), connected to a Thermo Element 2 spectrometer operated in low resolution mode ($m/\Delta m=300$). Analytical and data reduction procedures generally followed those described by Agranier and Lee (2007). Concentrations were determined on individual spots using a 44 µm-diameter laser beam (fig. 1) and a laser repetition rate of 10 Hz. The power output of the laser was approximately 15 J/cm^2. Transmission was typically estimated at about 10^5 cps/ppm of La in the BCR2 glass standard. Results were normalized to TiO_2 abundances measured by electron microprobe as an internal standard to account for variable ablation yield. For all data, the NIST 612 and BCR-2G glass standards were both used for external calibration of relative element sensitivities, using values given by Jochum et al. (2005). Replicate analyses of the USGS basaltic-glass standards BIR-1G and BHVO-2G run at intervals during the analytical session, yielded an external reproducibility generally better than 5 % (1σ relative standard deviation) at abundances similar to those found in impact spherules (Table 1).

3. Results and discussion

3.1 Bulk howardite and polymict eucrite samples

Howardites and polymict eucrites are extremely heterogeneous breccias. Obtaining a representative sample of a breccia would require crushing and homogenization of several grams of sample, depending on grain size and the proportion of clasts to matrix. It is generally not feasible to obtain such large amounts of a meteorite for bulk rock analysis. The major and trace element compositional variation displayed by howardites has been extensively reported in the literature (e.g., McCarthy et al., 1972; Chou et al., 1976; Fukuoka et al., 1977; Mittlefehldt et al., 1979; Palme et al., 1978), and the reader is referred to these previous studies for detailed discussion of the eucrite/diogenite mixing model and chondritic contribution. In this study, we have prepared "large" matrix samples (fine-grained portion devoid of large clasts (> 2-4 mm) of orthopyroxene or eucrite) weighing about 1 g. Four Saharan howardites were studied (NWA 1664, NWA 1769, NWA 5306, NWA 5614) and two polymict eucrites (NWA 5616 and 5618). Our aim was first to better characterize NWA 1664 and NWA 1769 using minor and trace element abundances (including the alkalis), oxygen isotope analysis, and then to compare these high-K glass-bearing samples with the other howardites .

3.1.1 Minor and trace elements

Bulk compositions of the six analyzed matrix samples of Saharan howardites and polymict eucrites are given in Table 2. In all cases the concentrations are in the range of previously analyzed HED polymict breccias (Mittlefehldt et al., 1998 and references therein). Ni abundances range from 12 to 125 µg/g and indicate a chondritic contribution of less than 1 wt%.

The six samples display flat CI-normalized rare earth (REE) patterns (La_n/Yb_n=1.1 to 1.2, fig. 2). Four of them (NWA 1664, 1769, 5306 and 5614) exhibit a similar negative Eu anomaly (Eu/Eu*=0.77 to 0.85). Interestingly, NWA 1664 and NWA 1769 matrices display virtually identical REE patterns and these resemblances extend to all the other analyzed elements (Table 2). Their Juvinas-normalized patterns are flat except for Cs and Rb enrichments, a feature which is well known in eucrites, in particular some main group-Nuevo Laredo eucrites (fig. 3). The patterns show no trace element enrichment that can be ascribed to hot desert secondary processes such as positive Ba or Sr anomalies (e.g., Barrat et al., 1999, 2001, 2003; Crozaz and Wadhwa, 2001). Indeed, these two samples display Ba/La, Sr/Nd, and Th/U ratios within the range measured in eucrite and howardite falls. This indicates, in agreement with petrographical observations, that these two samples are rather fresh, and the contribution from secondary phases to the trace element budget is negligible. Furthermore, the chemical differences between the two samples are so subtle, that they strongly suggest that these two howardites are paired. This inference is strengthened by the examination of the polished thick sections and the chemical composition of their fusion crust (Barrat et al., 2009a).

The other polymict breccias analyzed here exhibit the same type of Juvinas-normalized patterns as NWA 1664 and NWA 1769 but two of them (NWA 5306 and 5614) display marked positive Ba anomalies (Ba/La= 22 and 74, compared to approximately 10 in eucrite and howardite falls) which suggests that these two samples are much more weathered than the others examined in this study. Furthermore, with 27 ng/g Cs and 1 µg/g Rb, NWA 5614 is the Cs and Rb-richest sample studied here, and such an enrichment is most likely the result of terrestrial weathering. However, desert weathering is not the only explanation for these elevated values, as similarly high Rb and Cs abundances have previously been reported

in the matrix of the polymict eucrite Macibini (Buchanan et al., 2000), an observed fall. Notice that in both cases Li and Na abundances are unaffected by hot desert secondary processes.

3.1.2 Oxygen isotopes

Oxygen isotope results obtained in this study are given in Table 3 and plotted on figure 4a along with the previous HED results of Greenwood et al. (2005). All of the analyzed samples, plot on or within 3σ of the Eucrite Fractionation Line (EFL) ($\Delta^{17}O$ = -0.239 ± 0.007‰ (1σ), Greenwood et al. (2005)), consistent with them being isotopically normal HED meteorites (fig. 4a). Analyses of untreated polymict breccias form a relatively broad cluster that overlaps both the diogenite and eucrite fields on Fig. 4a; a feature that is consistent with the fact that howardites are a mixture of these two lithologies. The howardite samples show a slightly greater spread about the EFL than either eucrites or diogenites, which in part may reflect the fact that they sometimes contain non-HED materials (Mittlefehldt et al., 1998).

Deviation from the EFL could also be the result of terrestrial weathering. To test this possibility all samples were acid leached in 6M HCl for 30 minutes. The results for both leached and untreated samples are plotted on Fig. 4b. The untreated samples form a relatively broad cluster straddling the EFL, whereas those that have been acid leached form a more linear array, slightly displaced to higher $\delta^{18}O$ values compared to the untreated ones. Weathering in hot desert environments tends to shift samples to higher $\delta^{18}O$ values compared to their primary compositions (Greenwood et al., 2008). This is the opposite trend to that seen in figure 4b, where the leached samples, which should have a lower content of secondary minerals compared to the untreated samples, in fact have the highest $\delta^{18}O$ values. This suggests that the untreated howardites are relatively fresh and do not contain significant amounts of secondary minerals. In addition, the 6M HCl treatment is relatively harsh

compared to other leaching techniques commonly used used to remove secondary weathering products prior to oxygen isotope analysis (Greenwood et al., 2008). Consequently, the shift to higher $\delta^{18}O$ values seen in the acid leached samples may reflect some slight preferential removal of a primary low $\delta^{18}O$ phase such as orthopyroxene at the expense of plagioclase, which generally has slightly higher $\delta^{18}O$ values (Clayton, 1993).

3.2 High-K impact spherules

Among the score of spherules we have previously identified in NWA 1664 and 1769, only 17 were large and thick enough to be analyzed using our laser procedure. Depending on their size, we performed between one and three analyses per spherule-core, with the average for each spherule given in Tables 4 and 5. The spherules analyzed here cover the entire compositional range as established before (e.g., K_2O= 0.28 to 2.33 wt%, Barrat et al., 2009a), and display significant trace element variations.

3.2.1 Trace element abundances

High K glasses show an impressive range of Ni and Co abundances: from less than 5 to 31 µg/g for Co, and from 4 µg/g to 173 µg/g for Ni. These abundances are not correlated with MgO content, or any differentiation index. They are clearly related to small metal grains dispersed within the glasses. These concentrations make it possible to estimate the projectile contribution to the chemistry of the glasses. Assuming a chondritic composition, the projectile fractions never exceed 2 wt% in the glasses and hence contribute only a very negligible fraction to the major and trace element (apart from Ni and Co) inventories determined in this study.

CI-normalized REE patterns for the high-K impact spherules from NWA 1664 and NWA 1769 are presented in figure 5, and are in agreement with previous results (Kurat et al., 2003). The glasses display a significant range of REE abundances (e.g., La abundances vary from 1.7 to 4.9 µg/g, Yb from 1 to 2.6 µg/g, Tables 4 and 5). Their REE patterns are flat (La_n/Yb_n=1.05 – 1.56) and display negative to positive Eu anomalies (Eu/Eu*=0.77 – 1.17). They are similar to the patterns displayed by the howardites and eucrites, both in abundances and shapes. Indeed, REE abundances are correlated with MgO concentrations (fig. 6), and the spherule analyses straddle the howardite and eucrite fields. An immediate interpretation could be that the composition of the spherules can be explained by mixing of eucritic and diogenitic components, as expected for a regolith from Vesta. Although a similar conclusion is apparently suggested by the behavior of most of the refractory trace elements we have analyzed (REE, Zr, Hf, Sr, Nb, Ta, Th, U, and Ti), the reality is certainly more complex. The Juvinas-normalized patterns of high-K spherules are unlike those of howardites and eucrites (fig. 7), and display very distinct Ba, Li, K, Rb, Cs enrichments and deep Na anomalies, features which are unknown in either howardites or eucrites.

3.2.2 Are trace element abundances in high-K spherules pristine?

Ba in unweathered eucrites, being an incompatible, refractory element behaves like a light REE and as a consequence, the Ba/La ratio in this lithology is nearly constant and close to 10. Because diogenites display very low Ba and light REE abundances (e.g., Fukuoka et al., 1977; Palme et al., 1978; Mittlefehldt, 1994; Barrat et al., 2008), the Ba/La ratio in howardites is controlled by their eucritic components, and consequently is also close to 10 (fig. 8). High-K spherules are Ba-rich and their Ba/La ratios range from 16 to 112. It could be argued that these unusual values are not pristine but are the result of terrestrial weathering. As pointed out above (section 3.1.1), Ba is a good indicator of hot-desert weathering, and many

Saharan finds display high Ba concentrations. Indeed, Crozaz and Wadhwa (2001) have shown that glasses, as exemplified by some impact melt pockets in the highly weathered shergottite Dar al Gani (DAG) 476/489, were prone to enrichment in Ba by hot desert secondary processes. Nevertheless, this interpretation is not relevant to this study because:

(1) the howardites NWA 1664 and NWA 1769 are relatively fresh, and certainly much less weathered than DAG 476/489;

(2) unlike the DAG 476/489 impact melts the glasses do not show traces of weathering; their Sr abundances and Th/U ratios, which are other possible weathering indicators (e.g., Barrat et al., 2003), are not anomalous;

(3) and finally, Boesenberg and Mandeville (2007) have tried to determine the H_2O contents of two high-K spherules from NWA 1664 by Fourier transform infrared spectrometry (FTIR), and found no evidence of molecular H_2O, or OH. Although the behavior of water in impact glasses during hot desert weathering has yet to be investigated, it would seem highly likely that any significant interaction with terrestrial fluids during weathering would result in the presence of detectable traces of water, which is not the case...

High Li (29 to 93 µg/g), Rb (4.1 to 24.7 µg/g) and Cs (0.09 to 0.6 µg/g) abundances have been measured in high K spherules. As is the case for K (Barrat et al., 2009a), these high concentrations, are not affected by hot desert weathering. Li enrichments have yet to be observed in hot desert finds, and if some Rb can be introduced by alteration in hot desert meteorites, such a process could only account for a few tenths of a µg/g in the most weathered stones (e.g., DAG 476 (Barrat et al., 2001), or Dhofar 019 (Taylor et al., 2002)) and certainly not for several µg/g.

In contrast to other alkali elements and Ba, Na abundances in K-rich spherules are particularly low. Despite the large number of hot desert finds which have been studied in detail, some of which are strongly weathered, none show a depletion in Na abundance. Thus, these low abundances are certainly not a consequence of hot desert alteration.

We conclude that the remarkable patterns displayed by the high-K spherules found in NWA 1664 and NWA 1769 (fig.7) are pristine features and not the result of hot desert secondary processes.

3.2.3 Origin of the unusual trace element patterns of the high-K spherules

The contrasting alkali concentrations seen in high-K spherules and HEDs might lead one to suggest that they originated from distinct parent bodies. Howardites often contain exotic fragments (e.g., Gounelle et al., 2003, and references therein), and NWA 1664 or NWA 1769 are no exceptions (Lorenz et al., 2007). Unfortunately, due to their relatively small size (less than 0.03 mg for a typical spherule 200 µm in diameter) oxygen isotope analysis of individual spherules by laser fluorination is currently not possible. Furthermore, the current levels of precision available by ion-probe analysis are insufficient to resolve the very small differences in $\Delta^{17}O$ that separate many achondrite groups (i.e. isotopically normal and anomalous eucrites, angrites, brachinites, winonaites, pallasites and mesosiderites). Despite the present lack of oxygen isotope information, many observations enable us to infer that the high-K spherules formed on the same parent body as HEDs:

- it is now well established that basaltic achondrites derived from a number of parent bodies (Yamaguchi et al., 2001; Scott et al., 2008; Gounelle et al., 2009); the trace element abundances and the O isotopic compositions presented above confirm that NWA 1664 and NWA 1769 are true howardites, and are not related to the same parent

body as one of the isotopically anomalous eucrites, such as NWA 011, Pasamonte or Ibitira;

- the Fe/Mn ratios of the spherules are consistent with a link to the HEDs; moreover, the occurrence of an unmelted diogenitic remnant in a high K-spherule strongly strengthens this conclusion (Barrat et al., 2009a).

If the high-K spherules formed on Vesta, then two alternative formation scenarios need to be considered: firstly, they formed from normal HED targets but their compositions are not representative of their parent rocks, or have been modified by impact melting processes or during their flight; alternatively, they formed from targets whose compositions are unlike typical HEDs.

In terms of processes that might significantly alter the composition of spherules, alkali enrichment during incomplete melting of the target, and projectile contamination can be excluded (Barrat et al., 2009a), however, two opposing processes, evaporation and recondensation of volatile elements might be important.

In eucrites, Na abundances are controlled by plagioclase, and display the same behavior as Eu. Most eucrites, including the cumulate ones, have Na/Eu ratios around 5500 (when the concentrations are expressed in µg/g). Because of the low concentrations of both of these elements in diogenites, the eucritic fraction in howardites controls the Na and Eu budget. Thus, howardites plot on the same Na/Eu trend as eucrites (fig. 9). A few eucrites, however, display lower Na/Eu ratios. For example, ALHA 81001 exhibits a Na/Eu ratio as low as 2530 (Warren and Jerde, 1987; Scott et al., 2008), but such very low ratios are exceptions and not representative of the whole HED suite. The high-K spherules generally have a Na/Eu ratio

close to 1500. Taken at face value, this suggests that if the spherules were formed from HED targets, they have lost about 75 % of their Na through evaporation. If this inference is correct, elements more volatile or with the same volatility as Na, should have been affected in a similar manner. Instead, high-K spherules are not just significantly richer in K than any putative HED target, they have higher Rb and Cs values (fig. 7), which are much more volatile than Na (e.g., Gibson and Hubbard, 1972).

The discovery of the high Al, Si-poor (HASP) glasses in the Apollo 16 drill core have demonstrated that impacts can generate melts with bulk compositions very different to those of the melted targets, especially for the most volatile elements (Naney et al., 1976; Papike et al., 1997). Thus, it has often been assumed that the abundance of Na and other alkali elements in impact melts will not always closely match the composition of the target material (e.g., Delano et al., 1981). Whereas we do not dispute this argument, it is important to note that the behavior of alkalis during impact melting is often complex, and that significant losses of these elements do not follow a simple pattern, as shown by many examples of terrestrial (e.g., Humayun and Koeberl, 2004) or lunar impact glasses (e.g., Wentworth et al., 1994). Moreover, in the case of low-K impact spherules found in other howardites, Na abundances are well accounted for by mixing of selected eucrite and diogenite end members, suggesting that there has been no significant loss of this element from the majority of such spherules (Barrat et al., 2009a). We have generated many chemical maps and profiles across high-K spherules in order to detect evidence of alkali evaporation. In a few cases only, rims exhibit K depletion suggesting that some loss has taken place (fig. 10). Where such loss has taken place, it is restricted to the outer 30 µm (or less) of the spherules, and in consequence has not been analyzed for trace elements during the course of this study. Barrat et al. (2009a) have shown that apart from these K-depleted rims, the K abundance in the glassy objects from howardites

was not seriously affected by impact processes. The composition of the high-K glasses found in the howardites have been plotted on a Na_2O/MgO vs. CaO/MgO plot (fig. 11). Mg and Ca are both refractory elements (e.g., Delano et al., 1981). Hence, the CaO/MgO ratio should not be significantly fractionated by impact melting. On the other hand, the Na_2O/MgO ratio is highly sensitive to possible loss of Na during melting, or enrichment in Na via volatilisation/condensation processes. A selective Na-depletion should result in an erratic behavior of Na, and a strong decoupling of the refractory elements. A striking correlation for the NWA 1664 and NWA 1769 glasses is displayed on the diagram. This relationship suggests that Na has not been severely lost by the spherules during their formation. Similarly, this conclusion can be extended to the other alkalis.

It has been previously proposed that interaction between vapor and melt/glass can substantially enrich the latter in alkali metals. Delano (2005) has shown that some high-Ti picritic spherules found in Apollo 14 soils display substantial Na and K enrichments, and he ascribed this enrichment to a possible condensation of alkalis from the associated volcanic gases. However, such a process is unlikely to have operated in the case of the high-K impact spherules. It is an acknowledged fact that HEDs are K-poor. If vapors had been produced during impact into such targets, they will not have contained significant amounts of K. Unlike lunar volcanic glass beads (Meyer et al., 1975), the impact spherules found in howardites are not coated by condensates rich in alkali elements. The depletion in alkalis displayed by the rims of some of them strongly argue against any addition of K during their flight or subsequent cooling (fig. 10, and Barrat et al., 2009a).

A more complex process has been suggested for the alkali-rich clasts found in the Krähenberg and Bohla LL-chondritic breccias (Wlotzka et al., 1983). These clasts display

high enrichments of K (about 10 x), Rb (about 45 x) and Cs (about 70 x) relative to typical LL chondrites, while Na, Sr and Eu are strongly depleted (about 0.5 x), and the REE abundances are normal (except for a pronounced negative Eu anomaly). Wlotzka et al. (1983) proposed that these clasts formed from melts previously enriched in K, Rb, Cs, and that these features occurred as an exchange for Na in feldspars via a vapor phase. Although, these clasts share some unusual features with the high-K glasses found in howardites (e.g., high K/Na ratios), this mechanism is unlikely to be applicable to this study. Firstly, from an alkali content perspective, LL-chondrites and HEDs are hardly comparable. LL-chondrites contain twice as much Na as eucrites, and are thus much more prone to such exchange processes. Moreover, as pointed out by Wlotzka et al. (1983), this process does not severely affect the sum of Na + K atoms (Rb and Cs are insignificant here). Thus, a negative correlation between Na and the other alkalis should be observed. This is clearly not the situation for the high-K spherules: firstly, the most K-rich ones contain a much greater abundance of alkalis than even the most alkalis-rich potential HED target (e.g., the spherule A,2S found in NWA 1769 contain 3 x more alkali atoms than a eucrite); secondly, if this exchange process was operative, a strong negative correlation between Na and the other alkali elements would be expected; instead, Na abundances are positively correlated with Rb and other alkali abundances (fig. 12), ruling out this hypothesis.

Hence, the low-Na and high Li, K, Rb and Cs abundances displayed by the high-K impact spherules are not the fingerprints of complex processes that took place during the genesis of impact melts. They are more likely inherited from the targets. Indeed, the high Ba abundances and Ba/La ratios shown by all the high-K spherules cannot be achieved by impact processes, and strengthen this inference. An important question is the extent to which typical HED lithologies were present in the target material and how many end members are required

to explain the data? In agreement with the previous study (Barrat et al., 2009a), our trace element data suggest the involvement of specific lithologies.

The occurrence of a diogenite remnant in a K-rich impact spherule indicates unambiguously that this lithology was present in the target(s) (Barrat et al., 2009a). Furthermore, the involvement of a diogenitic-like component can adequately explain the spread of the data in the Yb vs. MgO diagram (fig. 6), or in the Na_2O/MgO vs. CaO/MgO diagram (fig. 11). In order to evaluate the possible role of eucritic components, the analyses of the spherules have been compared to eucrites and howardites in a Na/Eu vs. Rb/La plot (fig. 13). (Note that the dispersion seen in this diagram is insensitive to the participation of diogenites because these rocks have very low contents of Na, Rb, La and Eu compared to any "basaltic" component). The high-K spherules define a well-developed trend clearly distinct from the known eucrites and howardites. Moreover, this relationship points to the participation of at least two end members in addition to diogenites: a component with very low Na/Eu and Rb/La ratios (component A) and a second one with a very high Rb/La ratio (component B). The trend strongly suggests that typical eucrites which display Na/Eu>4000 are not required to explain the composition of the spherules. However, it should be noted, that the number of analyzed spherules is still low, and probably not sufficient to conclude definitively that this kind of rock is missing from the target(s) materials.

Unfortunately, we can only speculate about the possible parent lithologies of these two components, and their connections with diogenites. The first component could be a type of eucrite with extremely low Na abundances. It is entirely possible that such rocks could be present on Vesta. As pointed out above, ALHA 81001 an unusual eucrite with a low Na concentration has been identified, although its Na/Eu ratio (about 2530, Warren and Jerde,

1987) is higher than most high-K spherules. The second component could be a very high-K lithology. Indeed, a high-K felsic glass has been found in a spherule from NWA 1664 (SiO_2= 66.4 wt%, Al_2O_3=17.9 wt%, CaO=5.0 wt%, Na_2O=0.56 wt%, K_2O=5.8 wt%, Barrat et al., 2009a), but unfortunately was too small to be analyzed using our laser-ICP-MS procedure for trace elements. It should be noted that this Si-rich glass displays the same K_2O/Na_2O ratio (=10.4) as the spherule NWA1769A,2S which shows the highest K_2O abundance (K_2O/Na_2O=10.6), and this convergence is surely not fortuitous. Although such a component was certainly present in the target(s), its composition cannot explain satisfactorily the range of chemical compositions of the spherules (e.g., the K_2O abundances of the spherules are not correlated with the SiO_2 abundances), and requires a complex model. As an alternative, we suggest the following explanation. Assuming that lithologies of granitic composition are locally present in the crust, interactions between very-low Na basic melts (component A) and these "granitic" rocks are feasible, and can potentially generate melts with a "basaltic" composition and high Cs, Rb, K and Li abundances. A similar model has already been proposed for some lunar rocks. Small "granite" fragments have been recovered from lunar regoliths and breccias, and demonstrate that such rocks, although scarce, crop out on the Moon (see review in Papike et al., 1998). Debris of very high K basalts has been found in Apollo 14 breccias. These rocks could be generated from low-K basalts contaminated by these "granites" (Shervais et al., 1985; Neal et al., 1989). Interestingly, these very high K basalts are not only K rich and characterized by high K/Na ratios, but also like the lunar "granites" display high Rb abundances and high Ba/La ratios, a feature shared with the high K spherules found in the howardites. Interestingly, small amounts of a new high-K lithology have been found in the howardites NWA 1664 and NWA 1769 (Lorenz, 2008; Barrat et al., 2009b), and these could be remnants of the assumed high-K lithology (component B). These small fine-grained clasts are Mg-poor and made of a pyroxenoid breakdown product (fayalitic

olivine, hedenbergitic pyroxene, and silica), high-Ca pyroxene with exsolution lamellas, plagioclase, silica, hyalophane (K-Ba feldspar, with sometimes up to 10 wt% BaO), ilmenite, merrillite, apatite, zircon, baddeleyite, and troilite. Unfortunately, these rare clasts are very small (< 1 mm), and the studied surfaces cannot provide a correct estimate of their modes, nor of their chemical compositions. A more rigorous discussion of the origin of the Cs, Rb, K, Li, Ba enrichments and Na depletions shown by the high-K spherules must await the discovery of larger unmelted fragments of the target(s) ejected with the spherules.

4. Conclusions

The high-K impact spherules found in the NWA 1664 and NWA 1769 howardites are characterized by a high abundance of Cs, Rb, K, Li, and Ba, distinctive negative Na anomalies, while the REE and other refractory elements are unfractionated when normalized to the Juvinas eucrite (fig. 7). These remarkable patterns are unlike those of the host howardites, nor of other putative targets from Vesta. Because such features are pristine, and can hardly be the result of impact melting processes, we suggest that the high-K spherules formed on Vesta from unusual targets and were ballistically transported into their host breccias. The exact composition of the target is a matter of debate and cannot be fully constrained with the available data. They certainly contained a diogenitic component, but other end members are required: the minimum being a strongly-Na depleted eucrite-like component and a Cs, K, Rb, Li, and possibly Ba rich mafic component. Paradoxically, normal eucritic materials are not required to explain the compositional variation displayed by the K-rich impact spherules..

It is commonly accepted that the HED collection gives a fairly representative picture of the rocks exposed on the surface of Vesta. However, while our HED meteorite collection

is extensive (today it is on the order of 1000 different meteorites), it may be biased. Two lines of evidence point to this being the case. Firstly, cosmic-ray exposure ages for the HEDs suggest that all these meteorites are associated with only five impact events (Eugster and Michel, 1995; Welten et al., 1997), a number that is probably insufficient to sample all the geological diversity of the entire surface of the body. Secondly, despite the abundance of diogenites, and breccias that contain diogenitic debris (more than 40 % of the HED population), the parental melts of these orthopyroxenites have still not been recognized in the HED collection (e.g., Barrat et al., 2008). The high-K glasses found in some howardites which are formed from unusual targets, is a third line of evidence indicating that the lithological diversity of the Vesta's surface is much greater than commonly thought.

It is difficult to estimate the extent of the surface heterogeneity revealed by the K-rich impact spherules. K-rich glasses are now known from 5 unpaired breccias (LAP 04838, Luotolax, Macibini, Malvern, and NWA 1664/1769), and are not necessarily related to the same impact event. This suggests that the high-K areas on Vesta from which the glasses originated may be relatively extensive. The remote sensing of Vesta that will be performed from 2011 with the Dawn spacecraft, should allow the identification of chemically different areas on Vesta, and may help pinpoint the source regions of the K-rich impact glasses (Russell et al., 2007).

Acknowledgements

The samples analyzed during the course of this study were kindly provided by the Museum National d'Histoire Naturelle de Paris, Ahmed Pani, Philippe Thomas, Frederic Béroud and Ali Hmani. We thank Christian Koeberl for the editorial handling, Abhijit Basu and David Mittlefehldt for constructive comments, Philippe Gillet for fruitful discussions, and Pascale Barrat for her help. Gilles Chazot and Arnaud Agranier are thanked for their help with laser analyses. Jenny Gibson is thanked for her help with oxygen isotope analyses. We gratefully acknowledge the Programme National de Planétologie (CNRS-INSU) for financial support. IAF and RCG acknowledge support from STFC through a Rolling Grant to PSSRI. This research has made use of NASA's Astrophysics Data System Abstract Service.

References

Agranier A., Lee C.T.A. (2008) Quantifying trace element disequilibria in mantle xenoliths and abyssal peridotites. *Earth Planet. Sci. Lett*. **257**, 290-298;

Barrat J.A., Gillet Ph., Lesourd M., Blichert-Toft J., and Poupeau G.R. (1999) The Tatahouine diogenite: Mineralogical and chemical effects of sixty-three years of terrestrial residence. *Meteorit. Planet. Sci.* **34**, 91-97.

Barrat J.A., Blichert-Toft J., Gillet Ph., and Keller F. (2000) The differentiation of eucrites: the role of *in-situ* crystallization. *Meteorit. Planet. Sci.* **35**, 1087-1100.

Barrat J.A., Blichert-Toft J., Nesbitt R.W. and Keller F. (2001) Bulk chemistry of Saharan shergottite Dar al Gani 476. *Meteoritics Planet. Sci.* **36**, 23-29.

Barrat J.A., Jambon A., Bohn M., Blichert-Toft J., Sautter V., Göpel C., Gillet Ph., Boudouma O., and Keller F. (2003) Petrology and geochemistry of the unbrecciatted achondrite North West Africa 1240 (NWA 1240): an HED parent body impact melt. *Geochim. Cosmochim. Acta* **67**, 3959-3970.

Barrat J.A., Beck P., Bohn M., Cotten J., Gillet Ph, Greenwood R.C., and Franchi I.A. (2006) Petrology and geochemistry of the fine-grained, unbrecciatted diogenite Northwest Africa 4215. *Meteorit. Planet. Sci.* **41**, 1045-1057.

Barrat J.A., Yamaguchi A., Greenwood R.C., Bohn M., Cotten J., Benoit M., and Franchi I.A. (2007) The Stannern trend eucrites: contamination of main group eucritic magmas by crustal partial melts. *Geochim. Cosmochim. Acta* **71**, 4108-4124.

Barrat J.A, Yamaguchi A., Benoit M., Cotten J. and Bohn M. (2008) Geochemistry of diogenites : Still more diversity in their parental melts. *Meteoritics Planet. Sci* **43**, 1759-1775.

Barrat J.A., Bohn M., Gillet Ph., and Yamaguchi A. (2009a) Evidence for K-rich terranes on Vesta from impact spherules. *Meteorit. Planet. Sci.* **44**, 359-374.

Barrat J.A., Yamaguchi A., Greenwood R.C., Bollinger C., Bohn M., Jambon A., Boudouma O., and Franchi I.A. (2009b) High-K glasses and "KREEPy" clasts in howardites: evidence for K-rich terrane(s) on 4-Vesta. *Meteoritics Planet. Sci.* **44** (abstract, next met'soc meeting)

Buchanan P.C., Lindstrom D.J., Mittlefehldt D.W., Koeberl C., and Reimold W.U. (2000) The South African polymict eucrite Macibini. *Meteoritics. Planet. Sci*.**35**, 1321-1331.

Boesenberg J.S., Mandeville C.W. (2007) The driest glass in the Solar System: glass spherules in howardites. *Meteoritics Planet. Sci*., **42**, A20.

Chou C.L., Boynton W.V., Bild R.W., Kimberlin J., and Wasson J.T. (1976) Trace element evidence regarding a chondritic component in howardite meteorites. *Proc. Lunar Sci. Conf*. **7th**, 3501-3518.

Clayton R. N. (1993) Oxygen isotopes in meteorites. *Annu. Rev. Earth Planet. Sci*. **21,** 115-149

Crozaz G., Wadhwa M. (2001) The terrestrial alteration of Saharan shergottite Dar al Gani 476 and 489: a case study of weathering in a hot desert environment. *Geochim. Cosmochim. Acta* **65**, 971-978.

Delaney J.S., Prinz M., and Nehru C.E. (1982) Partial melt genesis for glassy clasts in basaltic achondrites. *Meteoritics* **17**, 204-205 (abstract)

Delano, J.W. (2005) Apollo 14 high-Ti picritic glass: oxidation/reduction by condensation of alkali metals. *Lunar Planet. Sci.* **36**, abstract #1081

Delano J.W., Lindsley. D.H., and Rudowski R. (1981) Glasses of impact origin from Apollo 11, 12, 15, and 16: evidence for fractional vaporization and mare/highland mixing. *Proc. Lunar Planet. Sci*, **12B**, 339-370.

Desnoyers C., Jérome J.Y.(1977) The Malvern howardite: a petrological and chemical discussion. *Geochim. Cosmochim. Acta* **41**, 81-86.

Drake M.J. (2001) The eucrite/Vesta story. *Meteoritics Planet. Sci.* **36**, 501-513.

Eugster O., Michel Th. (1995) Common break-up events of eucrites, diogenites, and howardites and cosmic-ray production rates for noble gases in achondrites. *Geochim. Cosmochim. Acta* **59**, 501-513.

Evensen N.M., Hamilton P.J. and O'Nions R.K. (1978) Rare Earth abundances in chondritic meteorites. *Geochim. Cosmochim. Acta* **42,** 1199-1212.

Fukuoka T., Boynton W.V., Ma M.S., and Schmitt R.A. (1977) Genesis of howardites, diogenites and eucrites. *Proc. Lunar Sci. Conf.* **8th**, 187-210.

Fuhrman M., Papike J.J. (1981) Howardites and polymict eucrites! Regolith samples from the eucrite parent body. Petrology of Bholgati, Bununu, Kapoeta, and ALHA76005. *Proc. Lunar Sci. Conf.* 12B, 1257-1279.

Gibson E.K., Hubbard N.J. (1972) Thermal volatilization studies on lunar samples. Proc. **3rd** Lunar Science Conf., (Supplement 3, Geochim. Cosmochim. Acta), 2, 2003-2014.

Gounelle M., Zolensky M.E., Liou J.C., Bland P.A., and Alard O. (2003) Mineralogy of carbonaceous chondritic microclasts in howardites: identification of C2 fossil micrometeorites. *Geochim. Cosmochim. Acta*, **67**, 507-527.

Gounelle M., Chaussidon M., Morbidelli A., Barrat J.A., Engrand C., Zolensky M.E., and McKeegan K.D. (2009) A unique basaltic micrometeorite expands the inventory of solar system planetary crusts. *PNAS*, **106**, 6904-6909.

Greenwood R.C., Franchi I.A., Jambon A., and Buchanan P.C. (2005) Widespread magma oceans on asteroidal bodies in the early solar system. *Nature* **435**, 916-918.

Greenwood R.C., Franchi I.A., Jambon A., Barrat J.A., and Burbine T.H. (2006) Oxygen isotope variations in stony-iron meteorites. *Science* **313**, 1763-1765.

Greenwood, R. C., Gibson J. M. and Franchi I. A. (2008) Hot and cold weathering: determining the oxygen isotope composition of achondrites *Workshop on Antarctic meteorites* abstract #4020.

Hewins R.H., Klein L.C. (1978) Provenance of metal and melt rock textures in the Malvern howardite. *Proc. Lunar Planet. Sci. Conf.* **9th**, 1137-1156

Humayun M. and Koeberl C. (2004) Potassium isotopic composition of Australasian tektites. *Meteoritics Planetary Sci.* **39**, 1509–1516.

Ikeda Y., Takeda H. (1984) Petrography and mineral compositions of the Yamato 7308 howardite. *Proc 9th Sympos. Antarctic Meteorites*, Nat. Inst. Polar Res., Tokyo, 149-183.

Jochum K.P., Willbold M., Raczeck I., Stoll B., and Herwig K. (2005) Chemical characterisation of the USGS reference glasses GSA-1G, GSC-1G, GSD-1G, GSE-1G, BCR2-G, BHVO2-G, and BIR1-G using EPMA, ID-TIMS, ID-ICP-MS and LA-ICP-MS. *Geostandards and Geoanalytical res*., **29**, 285-302.

Klein L.C., Hewins R.H. (1979), Origin of impact melt rocks in the Bununu howardite. *Proc. Lunar Planet. Sci. Conf.* **10th**, 1127-1140.

Kurat G., Varela M.E., Zinner E., Maruoka T., and Brandstätter F. (2003) Major, minor and trace elements in some glasses from the NWA 1664 howardite. *Lunar Planet. Sci. Conf*., **34**, (abstract #1733), CD ROM.

Labotka T.C., Papike J.J. (1980) Howardites: samples of the regolith of the eucrite parent-body: petrology of Frankfort, Pavlovka, Yurtuk, Malvern, and ALHA 77302. *Proc. Lunar Planet. Sci. Conf.* 11th, 1103-1130.

Lorenz C.A. (2008) Two possible sources of potassium bearing inclusions in the NWA 1664 howardite. *The 48-th Vernadsky/Brown Microsymposium on Comparative Planetology, Moscow, 20-22 October 2008 (abstract).*

Lorenz K.A., Nazarov M.A., Kurat G., Brandstätter F., and Ntaflos T. (2007) Foreign meteoritic material in howardites and polymict eucrites. *Petrology*, **15**, 115-132.

McCarthy T.S., Ahrens L.H., Erlank A.J. (1972) Further evidence in support of the mixing model for howardite origin. *Earth Planet. Sci Lett.* **15**, 86-93.

McCord T.B., Adams J.B., and Johnson T.V. (1970) Asteroid Vesta: spectral reflectivity and compositional implications. *Science* **168**, 1445-1447.

Meyer C. Jr, McKay D.S., Anderson D.H., and Butler P. Jr (1975) The source of sublimates on the Apollo 15 green and Apollo 17 orange glass samples. *Proc. Lunar. Sci. Conf.* **6th**, 1673-1699.

Miller M.F. (2002) Isotopic fractionation and the quantification of ^{17}O anomalies in the oxygen three-isotope system: an appraisal and geochemical significance. *Geochim. Cosmochim. Acta* 66:1881-1889.

Miller M. F., Franchi A., Sexton A. S. and Pillinger C. T. (1999) High precision $\delta^{17}O$ measurements of oxygen from silicates and other oxides: method and applications. *Rapid Commun. Mass Spectrom.* **13,** 1211–1217.

Mittlefehldt D.W. (1994) The genesis of diogenites and HED parent body petrogenesis. *Geochim. Cosmochim. Acta* **58**, 1537-1552.

Mittlefehldt D. W., Chou C.-L., and Wasson J. T. (1979) Mesosiderites and howardites; igneous formation and possible genetic relationships. *Geochim. Cosmochim. Acta* **43**, 673-688.

Mittlefehldt D. W. and Lindstrom M. M. (1997) Magnesian basalt clasts from the EET 92014 and Kapoeta howardites and a discussion of alleged primary magnesian HED basalts. *Geochim. Cosmochim. Acta* **61,** 453–462.

Mittlefehldt D.W., McCoy T.J., Goodrich C.A., and Kracher A. (1998) Non-chondritic meteorites from asteroidal bodies. In Planetary Materials, J.J. Papike, Ed. (Min. Soc. Am., *Reviews in Mineralogy* 36), chapter 4, 1-195.

Naney, M.T., Crowl, D.M., and Papike, J.J. (1976) The Apollo 16 drill core: Statistical analysis of glass chemistry and the characterization of a high alumina-silica poor (HASP) glass. *Proc. Lunar Sci. Conf*., **7th**, 155–184.

Neal, C.R., Taylor, L.A., Schmitt, R.A., Hughes, S.S., and Lindstrom, M.M. (1989) High alumina (HA) and very high potassium (VHK) basalt clasts from Apollo14 breccias, part 2: Whole rock chemistry: Further evidence for combined assimilation and fractional crystallization within the lunar crust. *Proceedings of the 19th Lunar Science Conference*, 147-161.

Noonan A.F. (1974) Glass particles and shock features in the Bununu howardite. *Meteoritics* **9**, 233-242.

Noonan A.F., Rajan S., Fredriksson K., and Nelen J. (1980) Chondrules in the Kapoeta and Bununu howardites. Lunar Planetary Institute, Houston, contribution #412, 139-140.

.

Palme H. et al. (1978) New data on lunar and achondrites and acomparaison of the least fractionated samples from the Earth, the Moon, and the eucrite parent body. *Proc. Lunar Planet. Sci. Conf.* **9th**, 25-37.

Papike J.J., Spilde M.N., Adcock C.T., Fowler G.W., and Shearer C.K. (1997) Trace-element fractionation by impact-induced volatilization: SIMS study of lunar HASP samples. *American Mineralogist* **82**, 630-634.

Papike J.J., Ryder G., and Shearer C.K. (1998) Lunar samples. In Planetary Materials, J.J. Papike, Ed. (Min. Soc. Am., *Reviews in Mineralogy* **36**, chapter 5, 1-234 (1998).

Russell C.T. et al. (2007) Dawn mission to Vesta and Ceres. *Earth, Moon and Planets*, **101**, 65, doi: 10.1007/s11038-007-9151-9 (2007).

Scott E.R.D., Greenwood R.C., Franchi I.A., Barrat J.A., and Sanders I. (2008) Oxygen isotopic constraints on the number and origin of basaltic achondrite parent bodies. *Lunar Planet. Sci. Conf.*, **39**, (abstract #2344)..

Shervais J.W., Taylor L.A., Laul J.C., Shih C.Y., and Nyquist L.E. (1985) Very high potassium (VHK) basalts: complications in mare basalt petrogenesis. *J. Geophys. Res*, **90**, supplement, D3-D18.

Takeda H. (1986) Mineralogy of Yamato 791073 with reference to crystal fractionation of the howardite parent body. Proc. 16th Lunar Planet. Sci. Conf., Part 2. *J. Geophys. Res.*, **91**, B4, D355-D363.

Taylor L. A., Nazarov M. A., Shearer C. K., McSween H. Y., Jr., Cahill J., Neal C. R., Ivanova M. A., Barsukova L. D., Lentz R. C., Clayton R. N., and Mayeda T. K. (2002) Martian meteorite Dhofar 019: A new shergottite. *Meteoritics Planet. Sci.* **37,** 1107–1128.

Tera F., Eugster O., Burnett D.S., and Wasserburg G.J. (1971) Comparative study of Li, Na, K, Rb, Cs, Sr and Ba abundances in achondrites and in Apollo 11 lunar samples. Proc. Apollo 11 Lunar samples Conf., Vol 2, 1637-1657.

Warren P.H, Jerde E. (1987) Composition and origin of Nuevo Laredo trend eucrites. *Geochim. Cosmochim. Acta* **51**, 713-725.

Welten K.C., Lindner L., Van der Borg K., Loeken T., Scherer P., and Schultz L. (1997) Cosmic-ray exposure ages of diogenites and the recent collisional history of the howardite, eucrite and diogenite parent body/bodies. *Meteoritics Planet. Sci.* **32**, 891-902.

Wentworth S.J., McKay D.S., Lindstrom D.J., Basu A., Martinez R.R., Bogard D.D., and Garrison D.H. (1994) Apollo 12 ropy glasses revisited. Meteoritics 29, 323-333.

Wlotzka F., Palme H., Spettel B., Wänke H., Fredriksson K., and Noonan A.F. (1983) Alkali differentiation in LL-chondrites. *Geochim. Cosmochim. Acta* **47**, 743-757.

Yagi K., Lovering J., Shima M. and Okada A. (1978), Mineralogical and petrological studies of the Yamato meteorites, Yamato-7301(j), -7305(k), -7308(l) and –7303(m) from Antarctica. *Proc. Symp. on Yamato Meteorites*, 2nd, 121-141.

Yamaguchi A., Clayton R.N., Mayeda T.K., Ebihara M., Oura Y., Miura Y.N., Haramura H., Misawa K., Kojima H., and Nagao K. (2002) A new source of basaltic meteorites inferred from Northwest Africa 011. *Science* **296**, 334-336.

Table 1. trace element compositions of international standards BIR-1G and BHVO-2G obtained by laser ICP-MS using a 44 µm-diameter laser beam (in µg/g). Literature data are from Jochum et al. (2005) excepted Li in BHVO-2 from Barrat et al. (2007)

	BIR-1G			**BHVO-2G**		
	n=4	RSD (%)	*literature*	n=4	RSD (%)	*literature*
Li	-	-		5.53	2.8	*4.7*
Ti	5874	(fixed)	*5874*	16663	(fixed)	*16663*
Co	56.3	3.4	*52.5*	45.8	1.1	*43*
Ni	192	0.7	*179*	132	2.0	*112*
Rb	0.31	15.4	*0.217*	9.58	2.7	*9.183*
Sr	115	3.6	*110*	412	1.4	*396*
Y	15.22	1.5	*16*	25.42	2.8	*29.2*
Zr	14.54	4.0	*17.8*	173	2.3	*172*
Nb	0.57	4.0	*0.535*	19.10	1.9	*18.2*
Cs	0.01	9.9	*0.005*	0.12	4.0	*0.102*
Ba	6.86	4.7	*6.8*	138	1.9	*132*
La	0.63	5.4	*0.607*	15.70	2.5	*15.25*
Ce	2.02	5.8	*1.88*	39.69	2.2	*37.67*
Pr	0.38	5.8	*0.376*	5.38	2.4	*5.33*
Nd	2.53	4.4	*2.4*	25.30	2.6	*24.55*
Sm	1.14	3.6	*1.09*	6.26	2.2	*6.119*
Eu	0.54	3.6	*0.524*	2.10	2.6	*2.077*
Gd	1.84	2.9	*1.85*	6.03	1.8	*6.125*
Dy	2.49	3.3	*2.64*	5.35	2.4	*5.281*
Er	1.63	3.2	*1.74*	2.52	4.0	*2.566*
Yb	1.63	1.9	*1.67*	1.99	2.4	*1.995*
Lu	0.23	1.8	*0.248*	0.27	3.7	*0.2766*
Hf	0.52	3.4	*0.62*	4.03	2.9	*4.22*
Ta	0.04	11.1	*0.038*	1.20	3.4	*1.08*
Th	0.03	8.9	*0.03*	1.20	2.4	*1.14*
U	0.02	18.5	*0.028*	0.45	3.4	*0.403*
(La/Sm)n	0.35	2.3	*0.35*	1.58	1.3	*1.57*
(La/Yb)n	0.26	3.7	*0.25*	5.33	1.2	*5.16*
Eu/Eu*	1.14	0.5	*1.13*	1.05	1.0	*1.04*
Ba/La	11.0	0.8	*11.2*	8.80	1.0	*8.66*

Table 2. Minor and trace element compositions of six Saharan howardites (*) and polymict eucrites (oxides in wt%, trace elements in µg/g).

	NWA 1664*	NWA 1769*	NWA 5306*	NWA 5614*	NWA 5616	NWA 5618
mass (g)	0.1195	0.1472	0.1053	0.1640	0.3521	0.1599
TiO_2	0.62	0.59	0.50	0.54	0.43	0.62
MnO	0.53	0.52	0.55	0.54	0.51	0.55
Na_2O	0.35	0.37	0.29	0.33	0.30	0.39
K_2O	0.05	0.03	0.04	0.08	0.03	0.04
Li	8.84	7.65	5.62	6.75	7.43	9.89
Be	0.21	0.23	0.15	0.19	0.13	0.21
Sc	27.9	27.5	22.8	27.1	14.0	27.9
V	85	82	119	84	93	90
Co	12.3	12.5	17.0	15.1	12.9	11.3
Ni	56.4	68.4	125	79.8	12.5	14.8
Cu	1.91	2.72	5.42	4.75	1.76	2.33
Zn	1.34	1.24	1.77	1.84	1.23	1.31
Ga	1.19	1.25	0.87	1.11	1.09	1.32
Rb	0.35	0.34	0.38	1.03	0.14	0.22
Sr	66.5	71.8	49.0	79.8	62.6	71.1
Y	16.90	16.71	10.73	15.24	10.51	14.38
Zr	46.4	43.1	29.2	36.1	27.5	37.2
Nb	3.95	3.61	3.14	3.05	2.38	3.54
Cs	0.014	0.018	0.012	0.027	0.007	0.009
Ba	27.35	30.52	38.17	191	19.27	24.76
La	2.79	2.79	1.75	2.59	1.87	2.29
Ce	7.15	7.19	4.46	6.68	4.77	5.87
Pr	1.07	1.07	0.682	0.993	0.710	0.893
Nd	5.45	5.42	3.44	5.02	3.58	4.46
Sm	1.76	1.73	1.10	1.58	1.12	1.42
Eu	0.520	0.559	0.327	0.466	0.450	0.531
Gd	2.36	2.36	1.48	2.16	1.51	1.99
Tb	0.422	0.417	0.263	0.378	0.270	0.351
Dy	2.75	2.74	1.76	2.47	1.79	2.31
Ho	0.600	0.601	0.381	0.541	0.391	0.504
Er	1.73	1.72	1.10	1.55	1.13	1.46
Yb	1.64	1.62	1.03	1.44	1.05	1.38
Lu	0.241	0.238	0.150	0.212	0.153	0.203
Hf	1.25	1.18	0.85	0.97	0.75	1.01
Ta	0.20	0.19	0.17	0.16	0.10	0.19
W	0.074	0.077	0.039	0.055	0.059	0.076
Th	0.340	0.368	0.221	0.331	0.193	0.285
U	0.091	0.103	0.094	0.081	0.060	0.082

Table 3. Oxygen isotopic compositions of six Saharan howardites (*) and polymict eucrites.

SAMPLE	n	$\delta^{17}O$‰	1σ	$\delta^{18}O$‰	1σ	$\Delta^{17}O$‰	1σ
UNTREATED SAMPLES							
NWA 1664*	1	1.629		3.596		-0.256	
NWA 1769*	1	1.689		3.649		-0.224	
NWA 5306*	2	1.571	0.065	3.494	0.085	-0.260	0.021
NWA 5614*	2	1.720	0.005	3.712	0.012	-0.226	0.011
NWA 5616	1	1.661		3.614		-0.233	
NWA 5618	1	1.679		3.678		-0.249	
ACID LEACHED SAMPLES (6M HCl)							
NWA 1664*	1	1.753		3.819		-0.249	
NWA 1769*	1	1.762		3.832		-0.246	
NWA 5306*	2	1.644	0.019	3.600	0.040	-0.243	0.002
NWA 5614*	2	1.795	0.074	3.882	0.131	-0.240	0.006
NWA 5616	1	1.889		4.072		-0.245	
NWA 5618	1	1.690		3.715		-0.257	

Table 4. Major and trace element compositions of 8 high-K spherules from howardite NWA 1664 (oxides in wt%, trace elements in µg/g).

	NWA1664 P,1S	NWA1664 P,3S	NWA1664 B1, 1S	NWA1664 B4,2S	NWA1664 B5,1S	NWA1664 B5,2S	NWA1664 B5,3S	NWA1664 B6,1S
TiO_2	0.60	0.33	0.73	0.58	0.54	0.65	0.57	0.40
MgO	10.61	16.39	8.34	10.28	11.75	8.93	13.18	16.89
Na_2O	0.09	0.10	0.20	0.14	0.09	0.18	0.08	0.14
K_2O	0.75	0.76	1.41	0.54	0.93	0.78	0.46	1.06
Li	35	43	81	45	43	50	39	69
Co	9.3	<5	<5	27.6	11.2	28.9	13.2	<5
Ni	39	12	4	111	54	108	39	4
Rb	7.55	5.36	14.66	10.63	7.70	9.65	5.46	12.28
Sr	54.7	54.0	120	84.2	63.9	81.6	67.6	60.1
Y	15.10	9.68	19.90	16.05	15.72	16.10	15.99	11.00
Zr	43.7	29.8	56.7	41.8	47.8	47.2	50.6	35.4
Nb	4.66	2.06	4.42	3.41	3.71	3.87	3.81	2.74
Cs	0.18	0.12	0.25	0.28	0.18	0.23	0.09	0.14
Ba	300	163	217	156	179	189	82.7	64.0
La	2.67	1.74	3.55	2.72	2.84	2.58	3.14	2.19
Ce	6.55	4.49	9.59	7.38	6.98	6.39	8.02	5.91
Pr	0.95	0.67	1.36	1.04	1.04	0.94	1.16	0.82
Nd	5.14	3.47	6.86	5.33	5.50	5.13	6.10	4.28
Sm	1.65	1.14	2.23	1.72	1.72	1.66	1.89	1.31
Eu	0.52	0.49	0.97	0.63	0.59	0.70	0.67	0.45
Gd	2.20	1.45	2.92	2.24	2.33	2.26	2.40	1.65
Dy	2.64	1.77	3.45	2.67	2.73	2.74	2.85	1.91
Er	1.54	1.07	2.17	1.67	1.62	1.70	1.69	1.15
Yb	1.41	0.99	2.07	1.64	1.50	1.66	1.60	1.10
Lu	0.21	0.15	0.30	0.23	0.23	0.24	0.23	0.16
Hf	1.01	0.78	1.51	1.05	1.18	1.20	1.25	0.85
Ta	0.22	0.11	0.22	0.15	0.20	0.21	0.20	0.13
Th	0.32	0.24	0.43	0.30	0.36	0.33	0.41	0.27
U	0.09	0.06	0.16	0.11	0.10	0.09	0.11	0.08
$(La/Sm)_n$	1.02	0.96	1.00	0.99	1.04	0.98	1.05	1.05
$(La/Yb)_n$	1.28	1.19	1.16	1.12	1.28	1.05	1.33	1.34
Eu/Eu*	0.84	1.16	1.17	0.98	0.90	1.10	0.96	0.93
Ba/La	112.16	93.42	61.07	57.39	62.85	73.12	26.36	29.17

Table 5. Major and trace element compositions of 9 high-K spherules from howardite NWA 1769 (oxides in wt%, trace elements in µg/g).

	NWA1769 A,1S	NWA1769 A,2S	NWA1769 A,3S	NWA1769 A,4S	NWA1769 A, 5S	NWA1769 A, 6S	NWA1769 A, 8S	NWA1769 C, 1S	NWA1769 C, 2S
TiO_2	0.63	0.46	0.50	0.63	0.55	0.67	0.91	0.56	0.62
MgO	11.63	15.43	16.03	11.84	13.11	8.45	5.95	12.99	9.53
Na_2O	0.14	0.22	0.05	0.29	0.10	0.20	0.27	0.11	0.16
K_2O	0.28	2.33	0.37	1.79	0.65	1.48	0.60	0.78	1.21
Li	33	81	29	93	37	73	58	51	62
Co	23.5	<5	30.7	16.0	15.7	9.8	<5	16.0	15.7
Ni	62	4	173	12	55	72	17	82	51
Rb	5.03	24.68	4.10	16.89	6.25	15.22	17.60	8.10	10.38
Sr	76.8	70.3	56.6	102.4	65.4	98.6	133.0	61.0	71.0
Y	17.55	13.02	14.84	16.66	16.06	19.24	26.44	14.02	15.69
Zr	49.55	42.41	47.19	50.51	52.50	55.39	73.14	44.57	53.01
Nb	3.87	3.35	3.91	4.14	4.42	4.24	5.66	3.76	4.55
Cs	0.11	0.60	0.09	-	0.12	0.28	0.47	0.18	0.27
Ba	92.4	205	66.3	53.6	87.3	139	171	118	131
La	3.13	2.79	3.09	3.22	3.43	3.49	4.94	2.96	3.47
Ce	8.51	7.46	8.48	8.98	9.39	9.41	13.33	8.15	9.81
Pr	1.18	1.03	1.14	1.23	1.28	1.28	1.85	1.14	1.32
Nd	6.07	5.21	5.81	6.25	6.53	6.62	9.46	5.85	6.95
Sm	1.90	1.46	1.74	1.93	1.92	2.07	2.95	1.79	1.99
Eu	0.71	0.43	0.53	0.65	0.58	0.77	0.99	0.57	0.60
Gd	2.50	2.02	2.21	2.45	2.45	2.73	3.80	2.18	2.44
Dy	3.01	2.27	2.54	2.87	2.80	3.26	4.47	2.60	2.76
Er	1.84	1.37	1.53	1.74	1.66	1.98	2.69	1.51	1.67
Yb	1.80	1.21	1.44	1.71	1.58	1.91	2.57	1.46	1.52
Lu	0.25	0.17	0.20	0.24	0.22	0.27	0.36	0.20	0.23
Hf	1.18	0.98	1.09	1.21	1.22	1.32	1.72	1.12	1.23
Ta	0.17	0.16	0.18	0.19	0.20	0.20	0.25	0.19	0.21
Th	0.33	0.31	0.34	0.36	0.39	0.38	0.51	0.38	0.43
U	0.10	0.10	0.09	0.09	0.10	0.13	0.16	0.11	0.15
(La/Sm)n	1.03	1.20	1.12	1.05	1.13	1.06	1.06	1.04	1.10
(La/Yb)n	1.17	1.56	1.45	1.27	1.46	1.23	1.30	1.37	1.54
Eu/Eu*	0.99	0.77	0.82	0.92	0.82	0.99	0.91	0.88	0.83
Ba/La	29.55	73.52	21.44	16.61	25.43	39.96	34.57	39.79	37.89

Figures captions

Fig. 1. Backscattered electron image of a glass spherule from the NWA 1664 howardite. Also shown are pits from two laser ICP-MS analyses.

Fig. 2. REE patterns of the Saharan howardites and polymict eucrites. The reference chondrite is from Evensen et al. (1978).

Fig. 3. Juvinas normalized element patterns of the Saharan howardites. Data for Juvinas, Nuevo Laredo and Stannern are from Barrat et al.(2007).

Fig. 4. (a) Oxygen isotope variation in treated and untreated howardites and polymict eucrites (this study) shown in relation to the HED, angrite and Main-Group pallasite data of Greenwood et al. (2005, 2006). D = diogenites. E = eucrites. H = howardites. TFL = terrestrial fractionation line. EFL = eucrite fractionation line ($\Delta^{17}O$ = -0.239±0.007(1σ) (Greenwood et al. (2005). (b) Oxygen isotope variation in untreated and acid leached howardites (this study). Untreated samples form a cluster centred on the EFL. Acid leached samples are shifted to higher $\delta^{18}O$ values indicating preferential removal of a low $\delta^{18}O$ phase.

Fig. 5. REE patterns of the high-K impact spherules found in howardites NWA 1664 and NWA 1769. The reference chondrite is from Evensen et al. (1978).

Fig. 6. Yb (µg/g) vs. MgO (wt%) plot for high K impact glasses from howardites NWA 1664 and NWA 1769. The fields for eucrites (E), cumulate eucrites (CE), diogenites (D), and howardites (H) are drawn from a compilation of literature data (see references in Mittlefehldt et al. (1998) and Barrat et al. (2007, 2008)).

Fig. 7. Juvinas normalized element patterns of the high-K impact spherules found in howardites NWA 1664 and NWA 1769. Data for Juvinas are from Barrat et al.(2007).

Fig. 8. Ba vs. La plot for high K impact glasses from howardites NWA 1664 and NWA 1769. The fields for unweathered eucrites (E), cumulate eucrites (CE), diogenites (D), and

howardites (H) are drawn from a compilation of literature data (see references in Mittlefehldt et al. (1998) and Barrat et al. (2007, 2008)).

Fig. 9. Na_2O (wt%) vs. Eu (µg/g) plot for high K impact glasses from howardites NWA 1664 and NWA 1769. The fields for eucrites (E), cumulate eucrites (CE), diogenites (D), and howardites (H) are drawn from a compilation of literature data (see references in Mittlefehldt et al. (1998) and Barrat et al. (2007, 2008)).

Fig. 10. Backscattered electron image and maps of Na, K, S and P of a spherule found in NWA 1769 that contains a rim devoid of K and a coating made of fine sulfide and phosphate grains.

Fig. 11. Na_2O/MgO vs. CaO/ MgO (wt%/wt%) for impact glasses from howardites (Noonan (1974), Desnoyers and Jérome (1977), Yagi et al. (1978), Hewins and Klein (1978), Klein and Hewins (1979), Noonan et al. (1980), Delaney et al. (1982), Ikeda and Takeda (1984)), and Barrat et al., 2009). The fields for eucrites (E), cumulate eucrites (CE), diogenites (D), and howardites are drawn from a compilation of literature data (see references in Mittlefehldt et al. (1998) and Barrat et al. (2007, 2008)).

Fig. 12. Li, Cs, K, Na vs. Rb plots for high K impact glasses from NWA 1664 and NWA 1769. The fields for HED are drawn from a compilation of literature data (mainly Tera et al. (1970), and Barrat et al. (2000, 2003, 2007)).

Fig. 13. Na/Eu vs. Rb/La (concentrations expressed in µg/g) plot for high K impact glasses from NWA 1664 and NWA 1769. The fields for howardites and eucrites are drawn from a compilation of literature data (see references in figure 11).

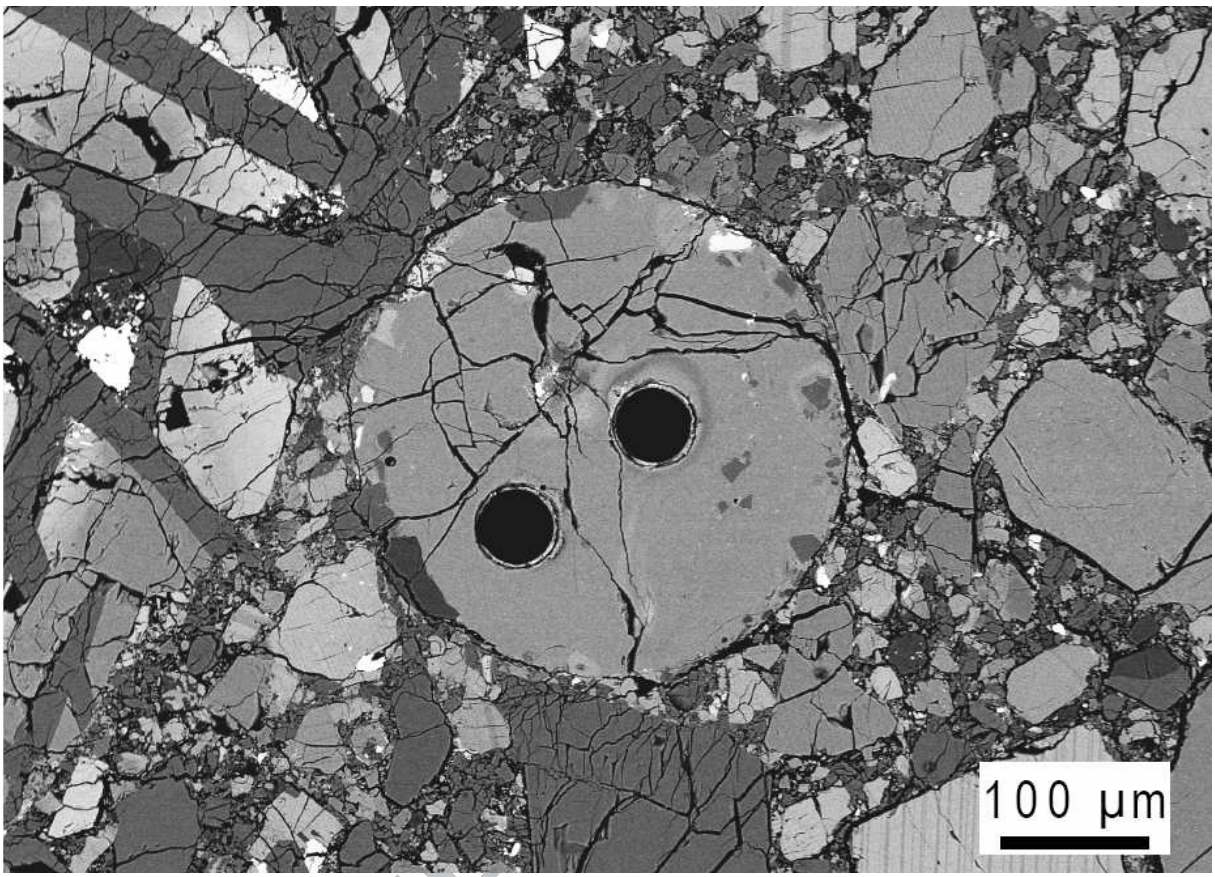

GCA W6381 fig1

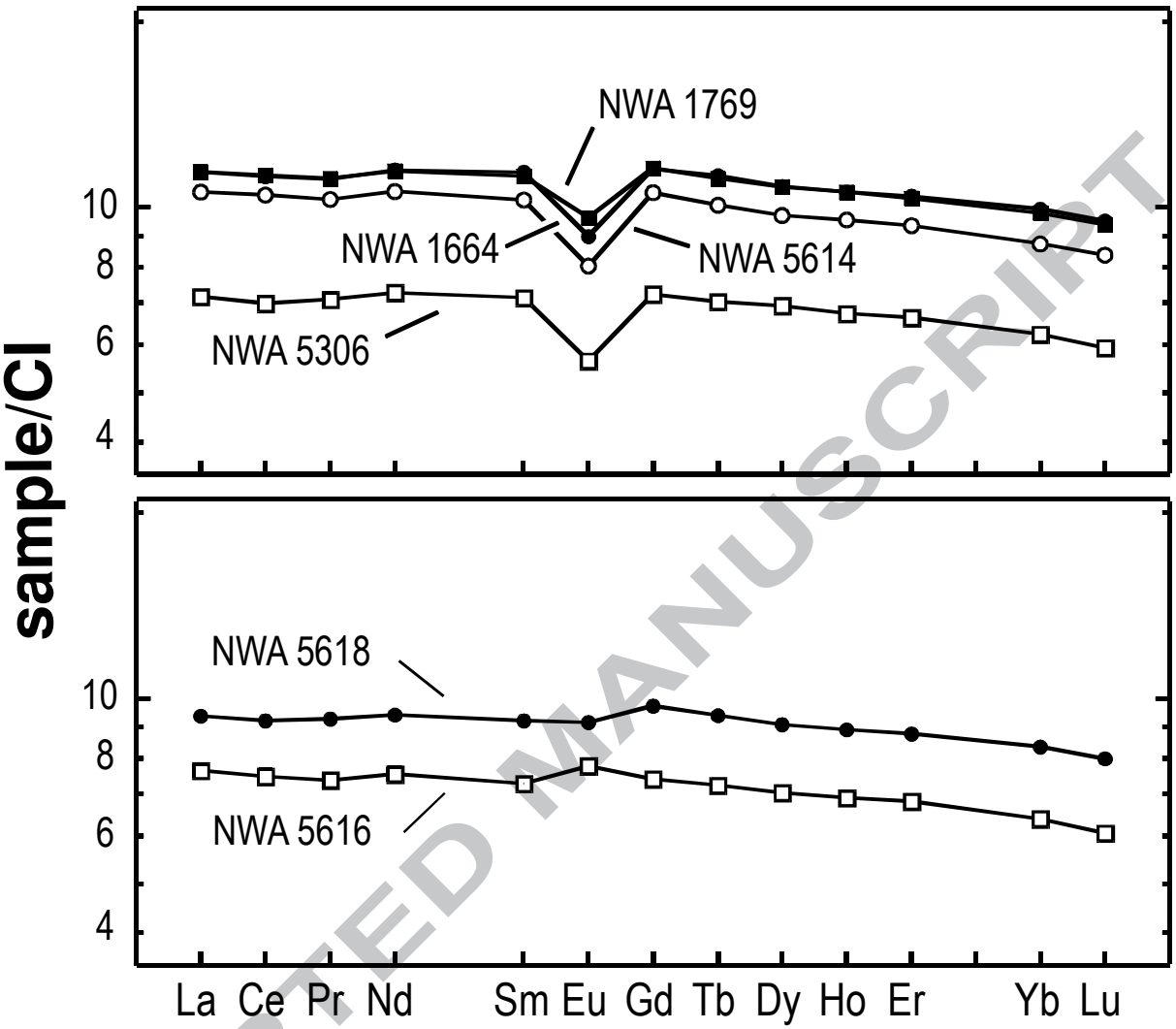

GCA W6381 fig 2

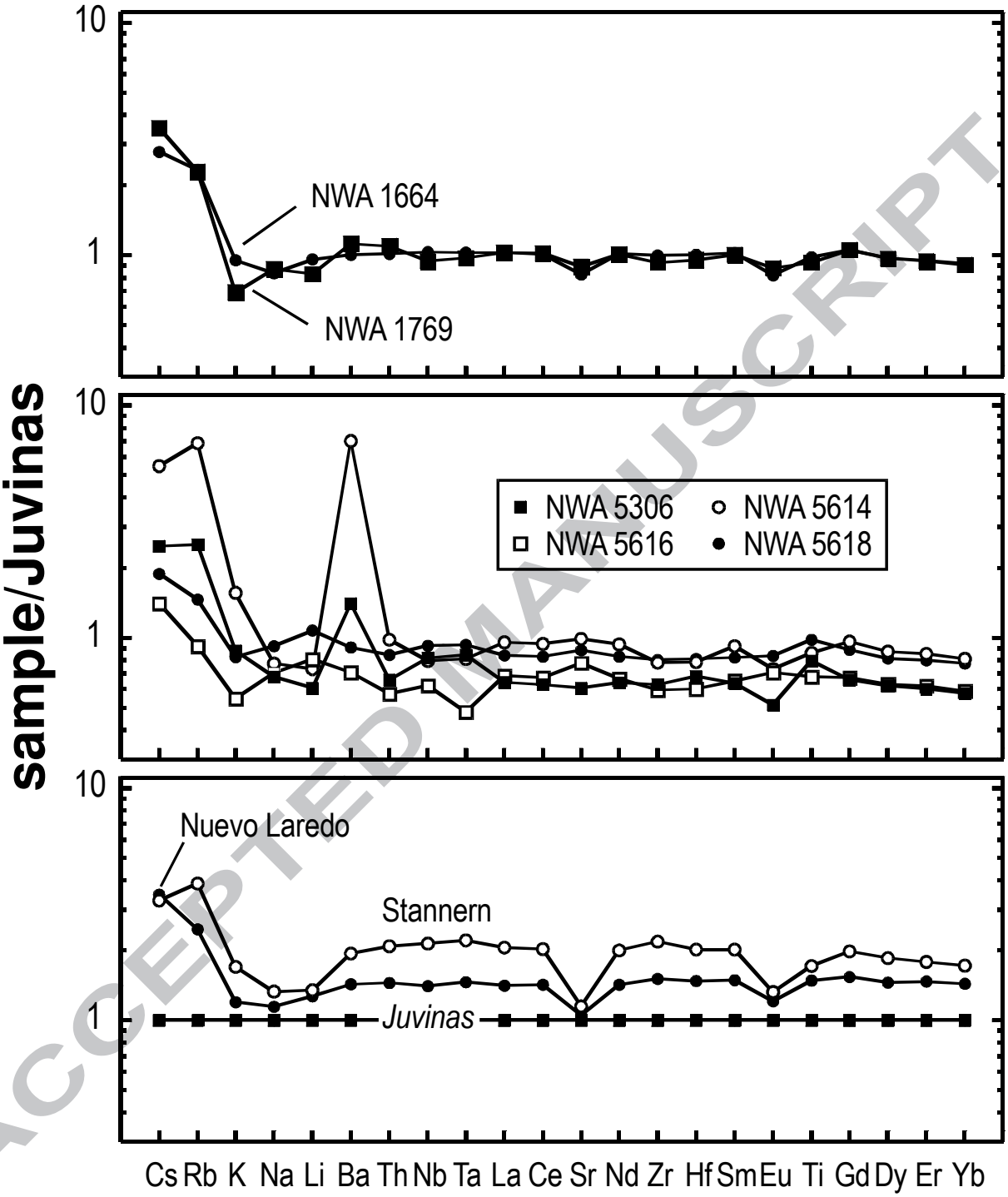

GCA_W6381_fig3

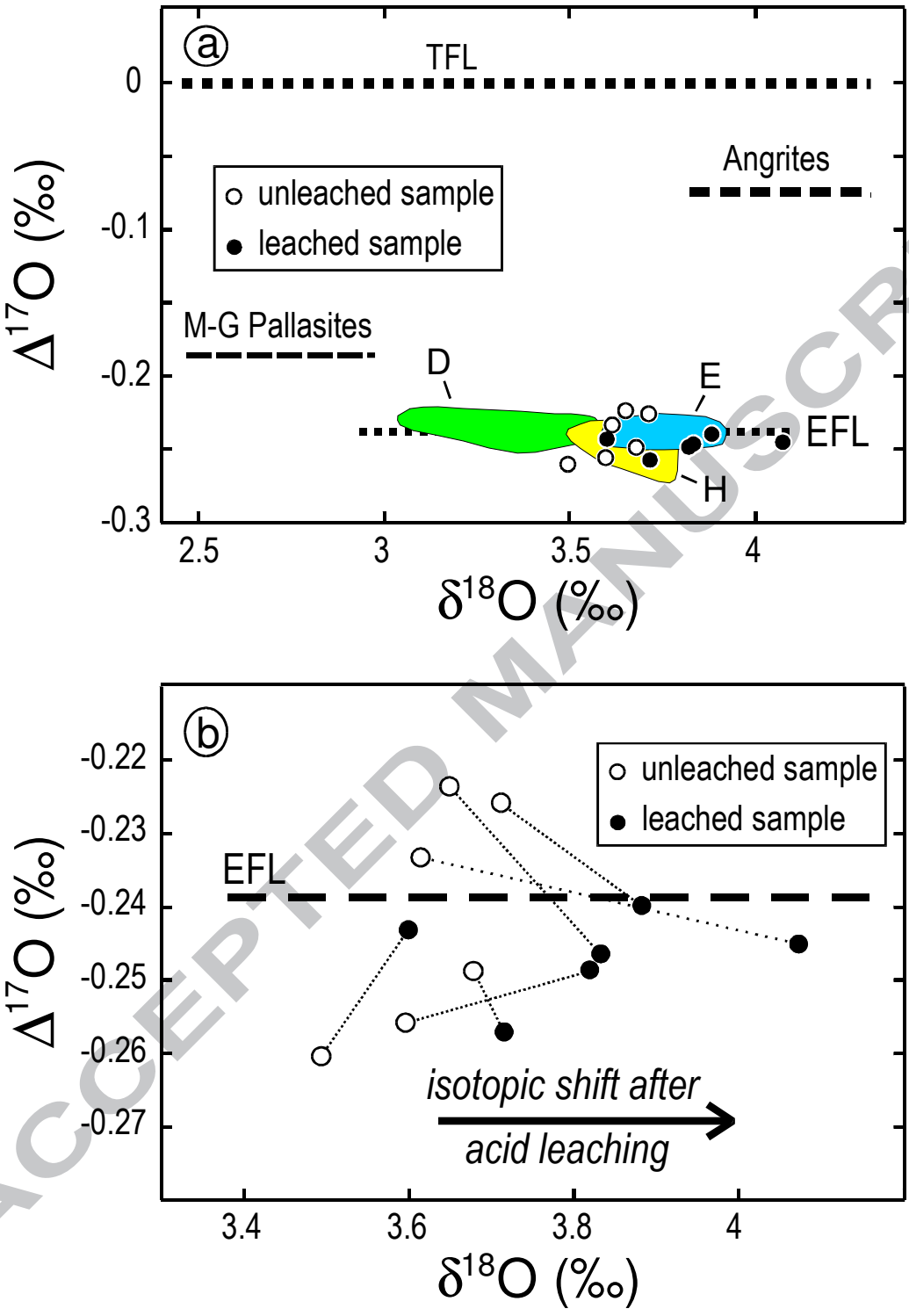

GCA W6381 fig4

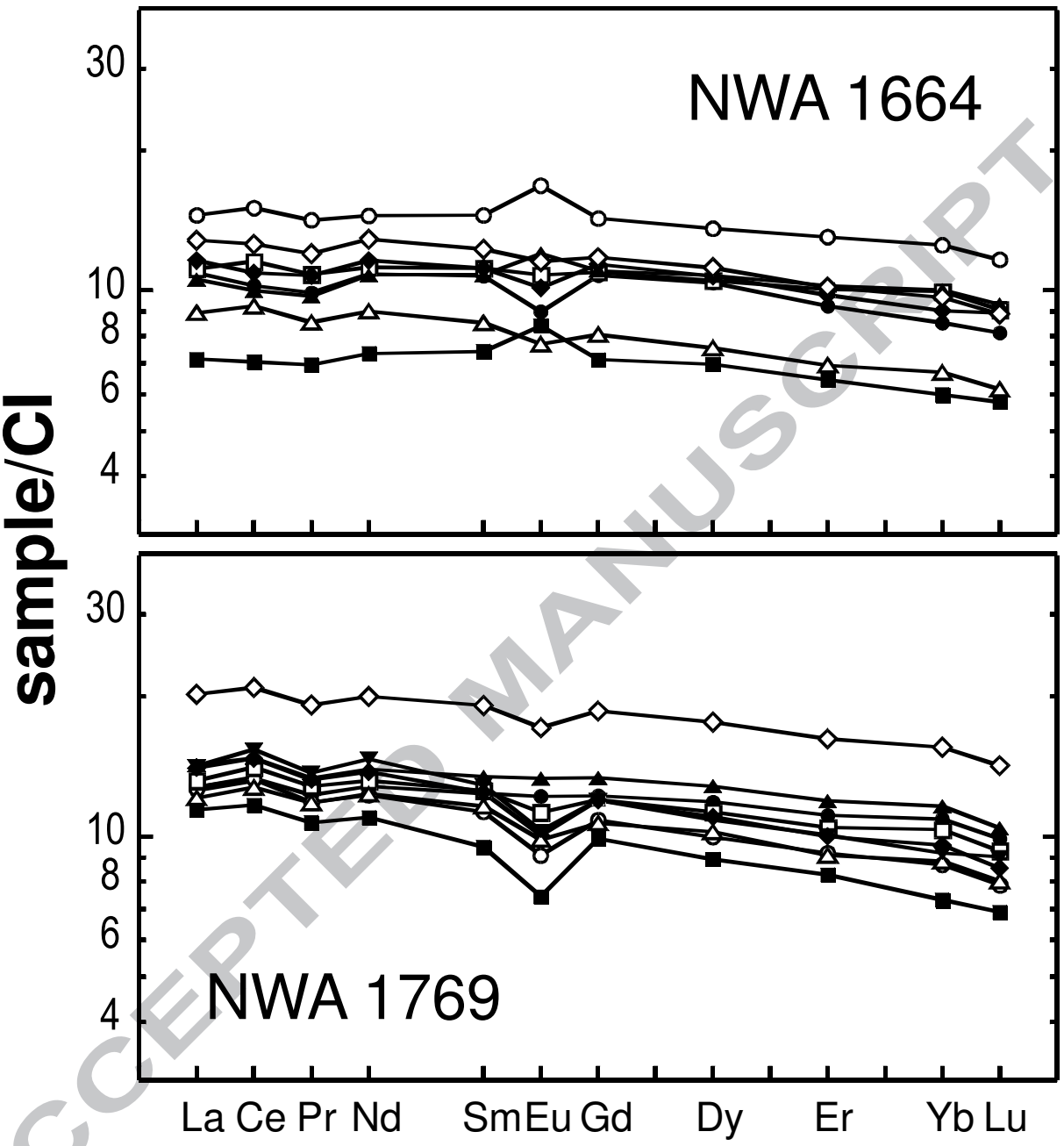

GCA W6381 fig5

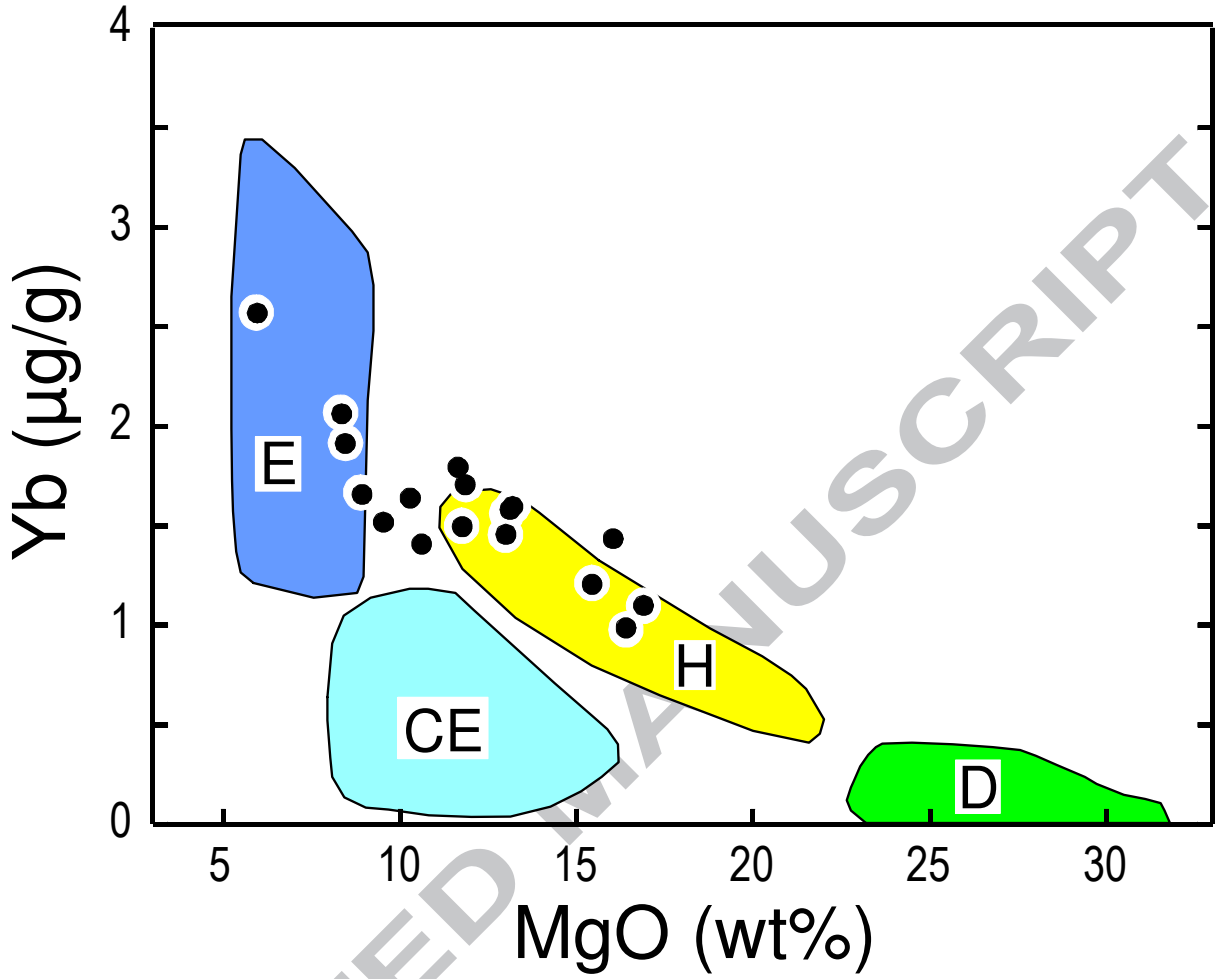

GCA W6381 fig6

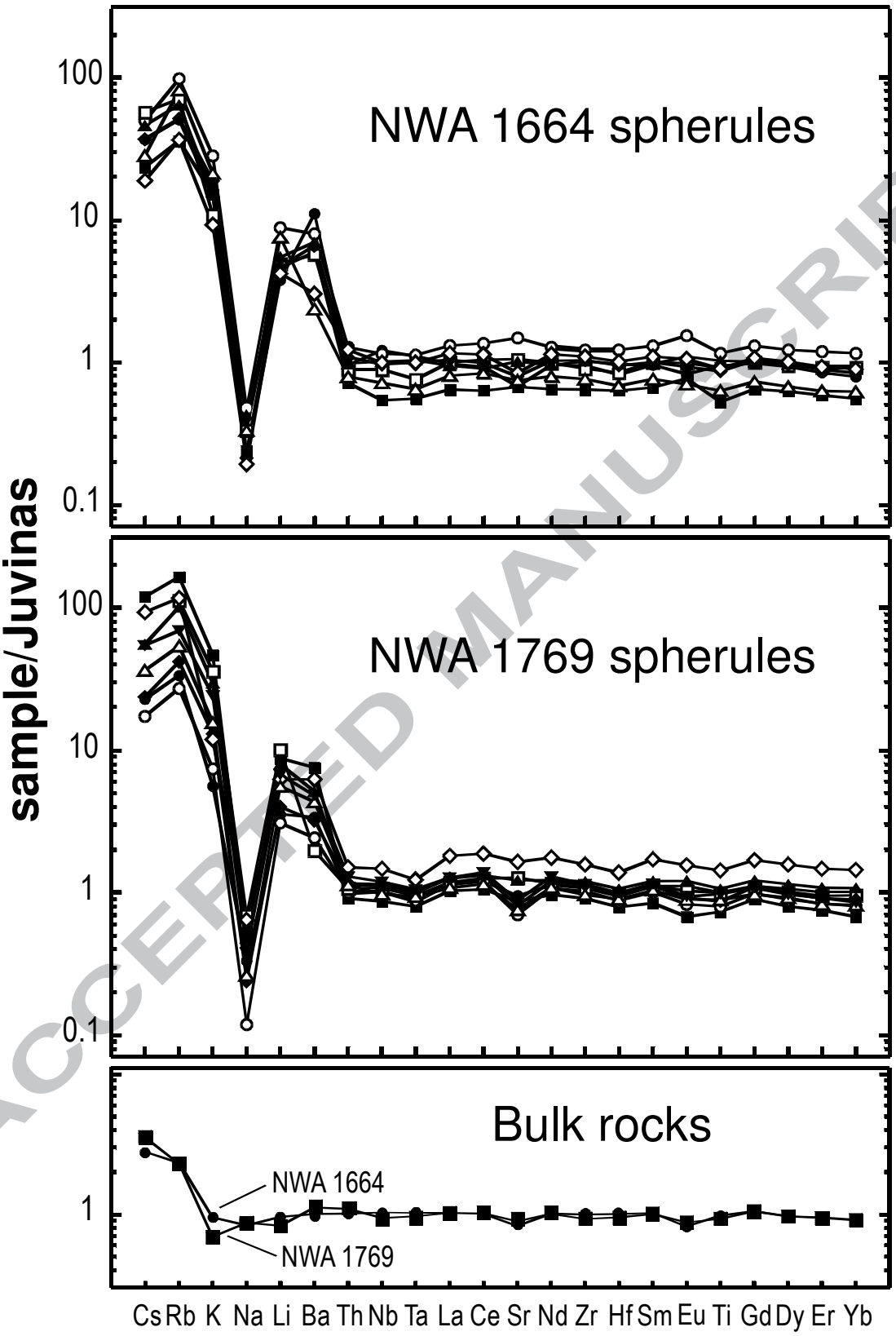

GCA W6381 fig7

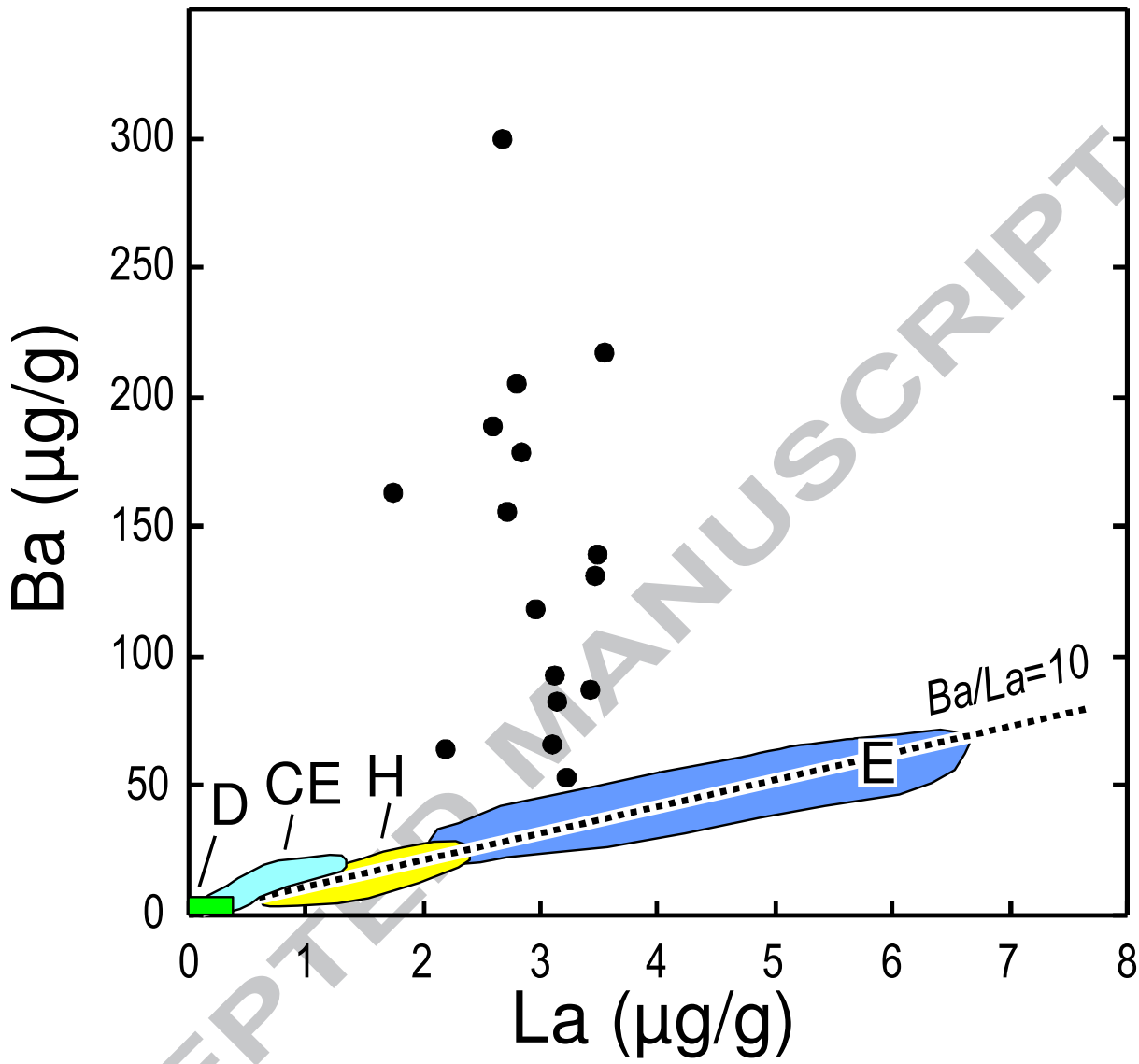

GCA W6381 fig8

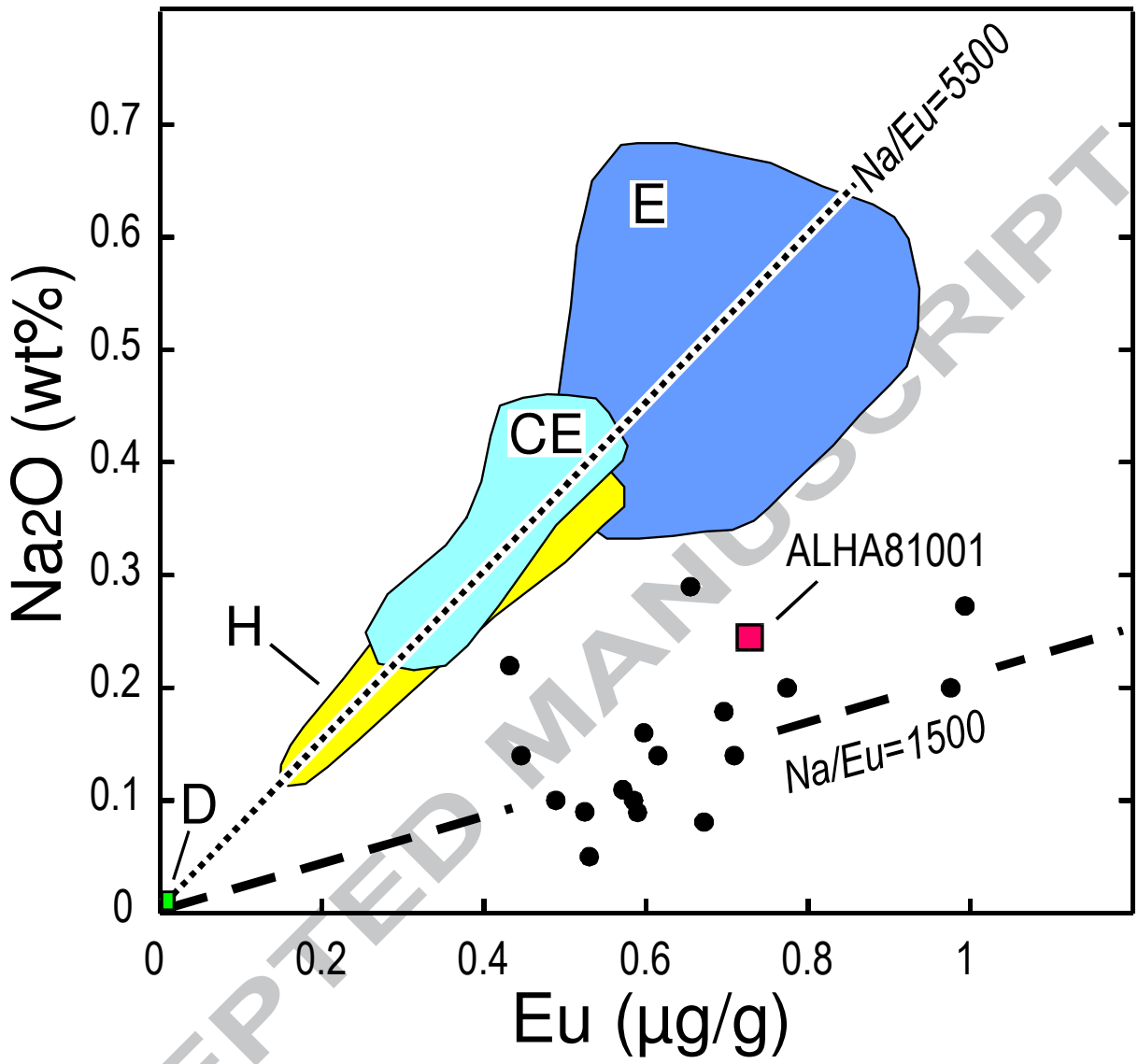

GCA W6381 fig9

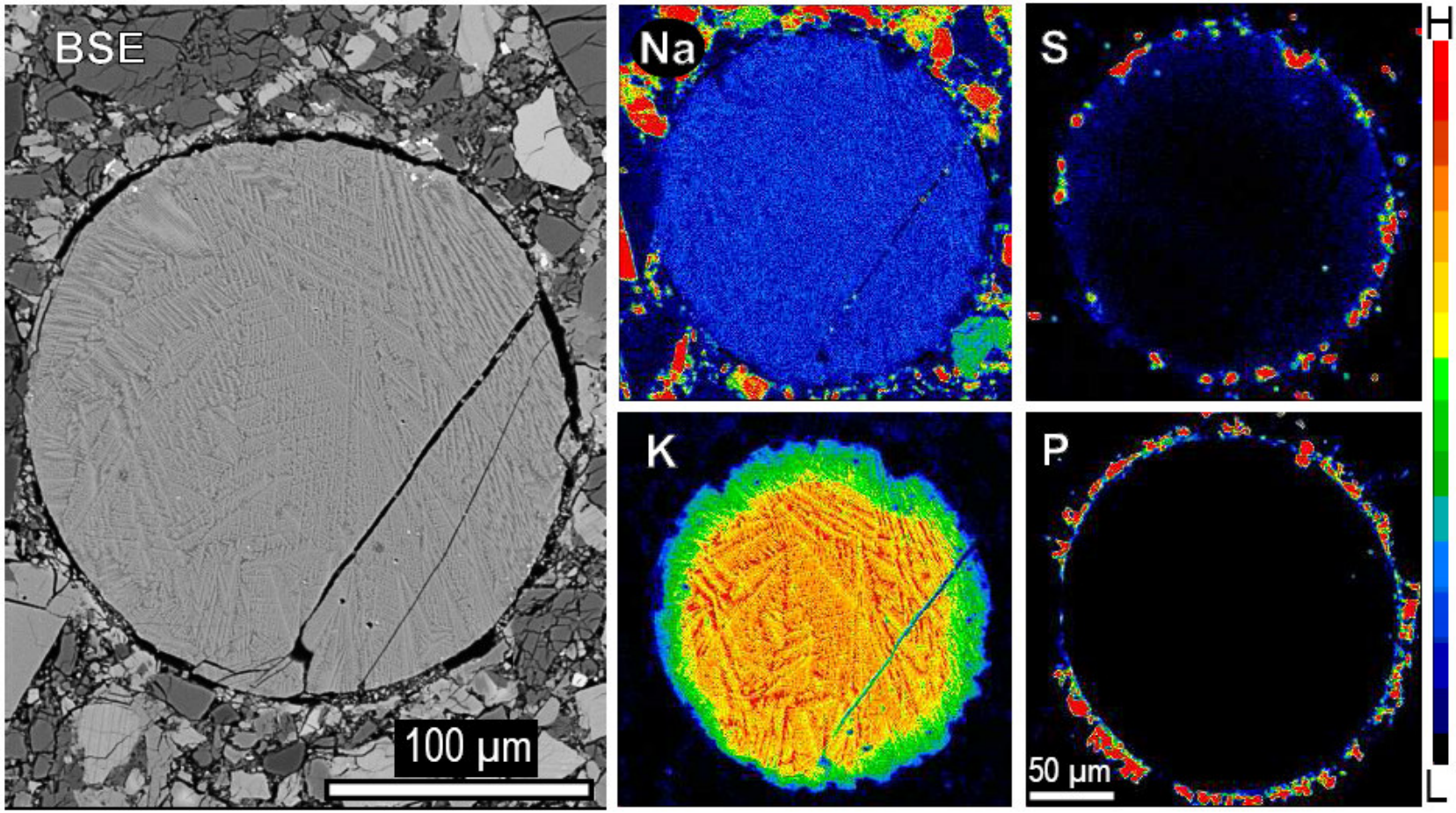

GCA W6381 fig10

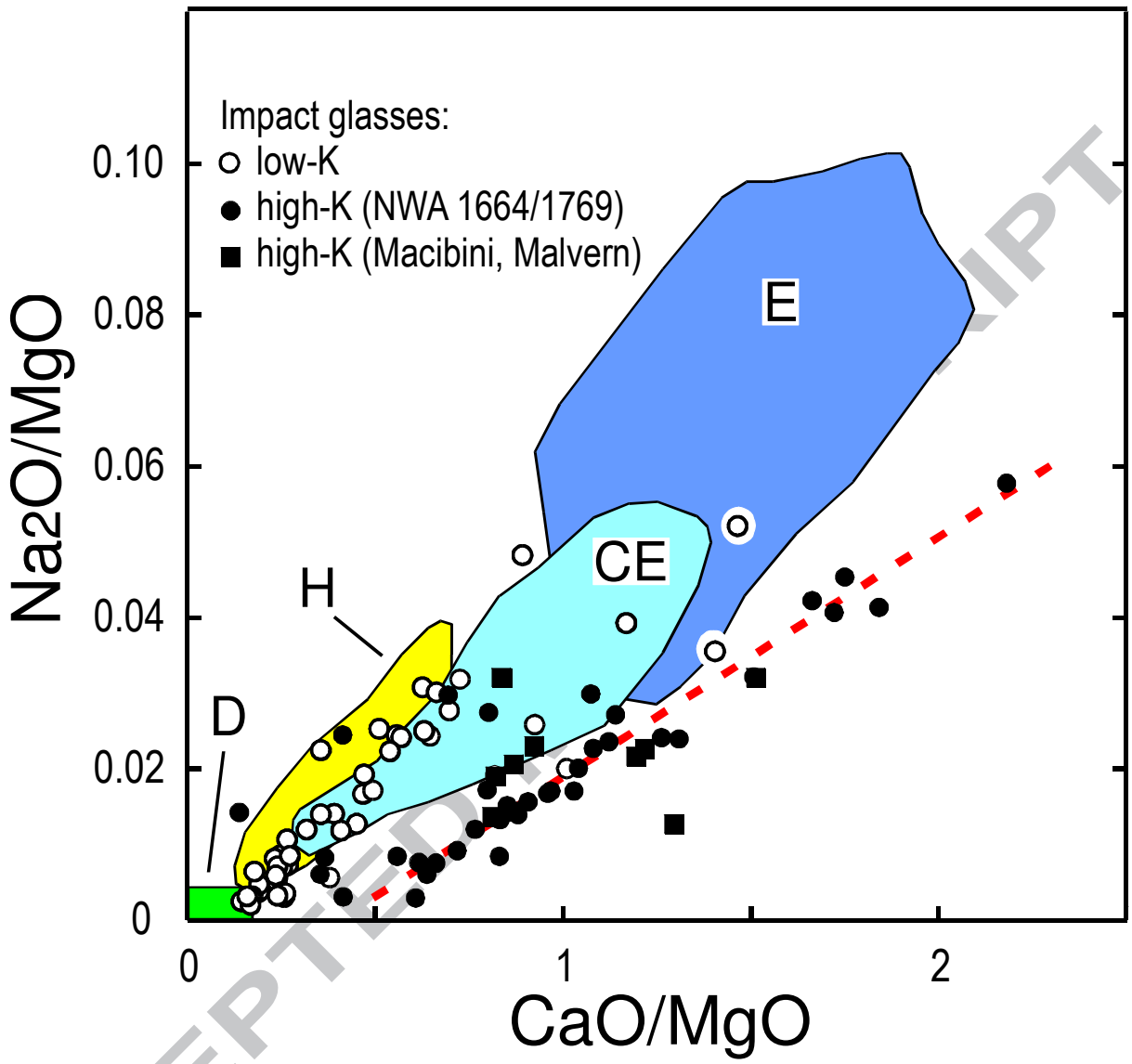

GCA W6381 fig11

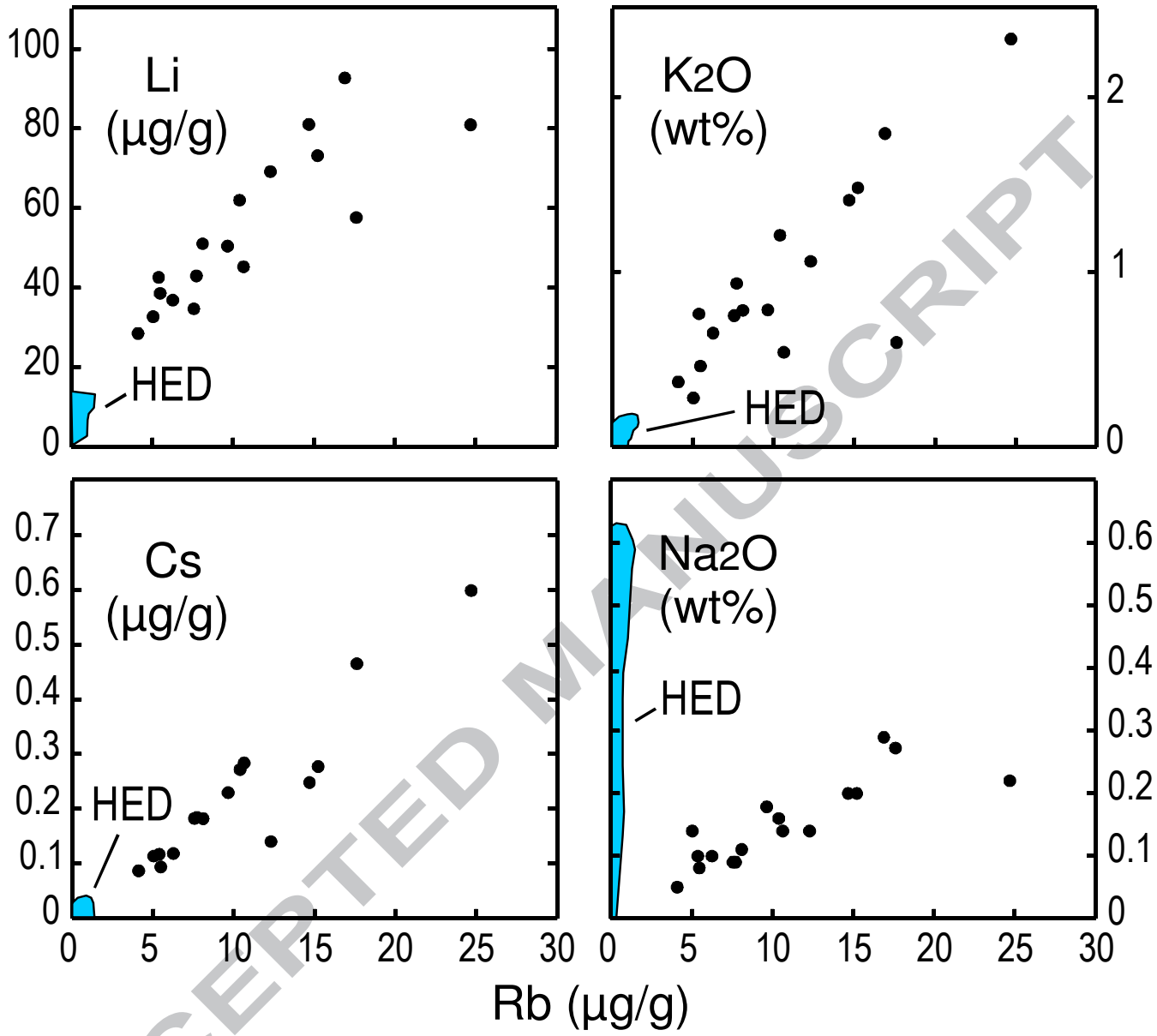

GCA W6381 fig12

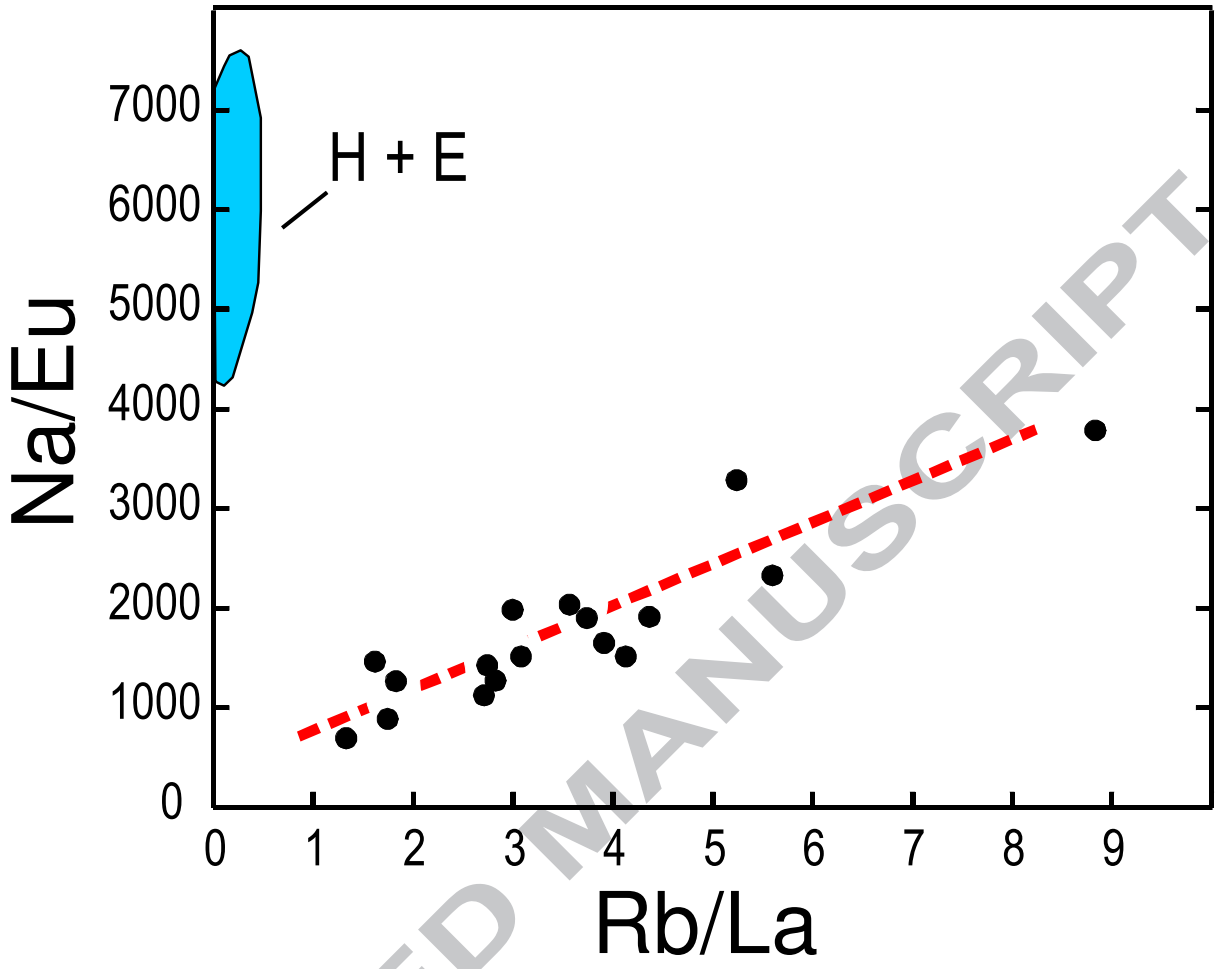

GCA W6381 fig13